



1 **The Open-source Data Inventory for Anthropogenic Carbon dioxide (CO<sub>2</sub>), version**  
2 **2016 (ODIAC2016): A global, monthly fossil-fuel CO<sub>2</sub> gridded emission data product for**  
3 **tracer transport simulations and surface flux inversions**

4  
5 Tomohiro Oda<sup>1,2</sup>, Shamil Maksyutov<sup>3</sup> and Robert J. Andres<sup>4</sup>

6  
7 1: Global Modeling and Assimilation Office, NASA Goddard Space Flight Center, Greenbelt,  
8 MD, USA.

9 2: Goddard Earth Sciences Technology and Research, Universities Space Research  
10 Association, Columbia, MD, USA

11 3: Center for Global Environmental Research, National Institute for Environmental Studies,  
12 Tsukuba, Ibaraki, Japan

13 4: Carbon Dioxide Information Analysis Center, Oak Ridge National Laboratory, Oak Ridge,  
14 TN, USA

15  
16 Corresponding author: T. Oda ([tomohiro.oda@nasa.gov](mailto:tomohiro.oda@nasa.gov))

17  
18 **Abstract**

19 Open-source Data Inventory for Anthropogenic CO<sub>2</sub> (ODIAC) is a global high-spatial  
20 resolution gridded emission data product that distributes carbon dioxide (CO<sub>2</sub>) emissions  
21 from fossil fuel combustion. The emission spatial distributions are estimated at a 1×1 km  
22 spatial resolution over land using power plant profiles (emission intensity and geographical  
23 location) and satellite-observed nighttime lights. This paper describes the latest version of the  
24 ODIAC emission data product (ODIAC2016) and presents analyses that help guiding data  
25 users, especially for atmospheric CO<sub>2</sub> tracer transport simulations and flux inversion analysis.  
26 Since the original publication in 2011, we have made modifications to our emission modeling  
27 framework in order to deliver a comprehensive global gridded emission data product. Major  
28 changes from the 2011 publication are 1) the use of emissions estimates made by the Carbon  
29 Dioxide Information Analysis Center (CDIAC) at Oak Ridge National Laboratory (ORNL)  
30 by fuel type (solid, liquid, gas, cement manufacturing, gas flaring and international aviation  
31 and marine bunkers), 2) the use of multiple spatial emission proxies by fuel type such as  
32 nightlight data specific to gas flaring and ship/aircraft fleet tracks and 3) the inclusion of  
33 emission temporal variations. Using global fuel consumption data, we extrapolated the  
34 CDIAC emissions for the recent years and produced the ODIAC2016 emission data product  
35 that covers 2000-2015. Our emission data can be viewed as an extended version of CDIAC  
36 gridded emission data product, which should allow data users to impose global fossil fuel  
37 emissions in more comprehensive manner than original CDIAC product. Our new emission  
38 modeling framework allows us to produce future versions of ODIAC emission data product  
39 with a timely update. Such capability has become more significant given the CDIAC's  
40 shutdown. ODIAC data product could play an important role to support carbon cycle science,  
41 especially modeling studies with space-based CO<sub>2</sub> data collected near real time by ongoing  
42 carbon observing missions such as Japanese Greenhouse Observing SATellite (GOSAT),  
43 NASA's Orbiting Carbon Observatory 2 (OCO-2) and upcoming future missions. The  
44 ODIAC emission data product is distributed from <http://db.cger.nies.go.jp/dataset/ODIAC/>  
45 with a DOI.

46  
47  
48



## 1 **1. Introduction**

2  
3 Carbon dioxide (CO<sub>2</sub>) emissions from fossil fuel combustion are the main cause for the  
4 observed increase in atmospheric CO<sub>2</sub> concentration. The Carbon Dioxide Information  
5 Analysis Center (CDIAC) at Oak Ridge National Laboratory (ORNL) estimated that the  
6 global total fossil fuel CO<sub>2</sub> emissions (FFCO<sub>2</sub>; fuel combustion, cement production and gas  
7 flaring) in the year 2014 was 9.855 PgC based on fuel statistics data published by United  
8 Nation (U.N.) (Boden et al., 2017). This FFCO<sub>2</sub> estimate often serves as a reference in carbon  
9 budget analysis, especially for inferring CO<sub>2</sub> uptake by terrestrial biosphere and oceans (e.g.  
10 Ballantyne et al., 2012; Le Quéré et al., 2016). The Global Carbon Project for example  
11 estimated that approximately 55% of the carbon released to the atmosphere (FFCO<sub>2</sub> plus  
12 emissions from land use change) was taken up by natural sinks over the past decade (2006-  
13 2015) (Le Quéré et al., 2016).

14 Similarly, FFCO<sub>2</sub> estimates serve as a reference in atmospheric CO<sub>2</sub> flux inversion analysis  
15 where the location and size of natural sources and sinks are estimated using atmospheric CO<sub>2</sub>  
16 data and atmospheric transport models (e.g. Tans et al., 1990; Bousquet et al., 1999; Gurney  
17 et al., 2002; Baker et al., 2006). In the conventional inversion method, unlike land and  
18 oceanic fluxes, FFCO<sub>2</sub> is a given quantity and never optimized (e.g. Gurney et al., 2005).  
19 FFCO<sub>2</sub> thus needs to be accurately quantified and given in space and time to yield robust  
20 estimates of natural fluxes (Gurney et al., 2005). Accurately prescribing FFCO<sub>2</sub> has become  
21 more critical because of the use of spatially and temporally dense CO<sub>2</sub> data from a wide  
22 variety of observational platforms (ground-based, aircrafts and satellites), which inform not  
23 only background levels of CO<sub>2</sub> concentration, but also CO<sub>2</sub> contributions from anthropogenic  
24 sources (e.g. Schneising et al., 2013; Janardanan et al., 2016; Hakkarainen et al., 2016).  
25 Atmospheric transport models then need to be run at a higher spatiotemporal resolution than  
26 before to fully interpret and utilized CO<sub>2</sub> variability observed at synoptic to local scale to  
27 quantify sources and sinks (e.g. Feng et al. 2016; Lauvaux et al., 2016). FFCO<sub>2</sub> data thus  
28 needs to be accurately given at a high resolution so as not to cause biases in simulations.

29 Global FFCO<sub>2</sub> data are available in a gridded form from different institutions and research  
30 groups (e.g. CDIAC/ORNL and Europe's Joint Research Center (JRC)) and those gridded  
31 emission data are often based on disaggregation of national (or sectoral) emissions (e.g.  
32 Andres et al., 1996; Rayner et al., 2010; Oda and Maksyutov 2011; Janssens-Maenhout et al.,  
33 2012; Kurokawa et al., 2013; Asefi-Najafabady et al., 2014). The emission spatial  
34 distributions are often estimated using spatial proxy data that approximate the location and  
35 intensity of human activities (hence, CO<sub>2</sub> emissions) (e.g. population, nighttime lights and  
36 gross domestic production (GDP)) and/or geolocation of specific emission sources (e.g.  
37 power plant, transportation, cement production/industrial facilities and gas flares). CDIAC  
38 gridded emission data product for example is based on an emission disaggregation using  
39 population density at a 1×1 degree resolution (Andres et al., 1996). The Emission Database  
40 for Global Atmospheric Research (EDGAR, <http://edgar.jrc.ec.europa.eu/>) estimates  
41 emissions on the emission sectors specified by the Intergovernmental Panel on Climate  
42 Change (IPCC) methodology instead of fuel type and use spatial proxy data and geospatial  
43 data such as point and line source location at a 0.1×0.1 degrees (Janssens-Maenhout et al.,  
44 2012).

45 Satellite-observed nighttime light data has been identified as an excellent spatial indicator  
46 for human settlements and intensities of some specific human activities (e.g. Elvidge et al.,  
47 1999, 2009) and has been used to infer the associated CO<sub>2</sub> emissions or their spatial  
48 distributions (e.g. Doll et al., 2000, Ghosh et al., 2010, Rayner et al., 2010). Oda and



1 Maksyutov (2011) proposed a combined use of power plant profiles (power plant emission  
2 intensity and geographical location) and nighttime light data to achieve a global high-spatial  
3 resolution emission field. The decoupling of the point source emission which often have less  
4 spatial correlation with population (hence, nighttime light), yields an improved high-  
5 resolution emission field that shows an improved agreement with the U.S. 10km Vulcan  
6 emission product developed by Gurney et al. (2009) (Oda and Maksyutov 2011). Based on  
7 Oda and Maksyutov (2011), we initiated a high-resolution emission data development (named  
8 as the Open-source Data Inventory for Anthropogenic CO<sub>2</sub>, ODIAC) under the Japanese  
9 Greenhouse Gases Observing SATellite (GOSAT, Yokota et al., 2009) at the Japanese  
10 National Institute for Environmental Studies (NIES). The original purpose of the emission  
11 data development was to provide an accurate prior FFCO<sub>2</sub> field for global and regional CO<sub>2</sub>  
12 inversions using the column-averaged CO<sub>2</sub> (X<sub>CO<sub>2</sub></sub>) data collected by GOSAT. Since 2009, the  
13 ODIAC emission data product has been used for the inversion for the official GOSAT Level  
14 4 (surface CO<sub>2</sub> flux) data production (Takagi et al., 2009; Maksyutov et al., 2013), NOAA's  
15 CarbonTracker (Peters et al., 2007) as a supplementary FFCO<sub>2</sub> data, as well as dozens of  
16 published works (e.g. Saeki et al., 2013; Thompson et al., 2015; Feng et al., 2016; Feng et al.,  
17 2017; Shirai et al., 2017) including several urban scale modeling studies (e.g. Ganshin et al.  
18 2010; Oda et al., 2012; Brioude et al., 2013; Lauvaux et al., 2016; Janardanan et al., 2016;  
19 Oda et al., 2017).

20 In response to increasing needs from the CO<sub>2</sub> modeling research community, we have  
21 upgraded and modified our modeling framework in order to produce a global, comprehensive  
22 emission data product on timely manner, while our flagship high-resolution emission  
23 modeling approach remains as the same. In this manuscript, we describe the latest version of  
24 the ODIAC emission data product (ODIAC2016, 2000-2015) along with the emission  
25 modeling framework we are currently based on, highlighting changes/differences from Oda  
26 and Maksyutov (2011).

27

28

## 29 **2. Emission modeling framework**

30

31 Fig. 1 illustrates our current ODIAC emission modeling framework (we defined it as  
32 "ODIAC 3.0 model", in contrast to the original version). Major changes/differences from Oda  
33 and Maksyutov (2011, ODIAC v1.7) are 1) the use of emissions estimates made by the  
34 CDIAC (rather than our own emission estimates), 2) the use of multiple spatial emission  
35 proxies in order to distribute CDIAC emissions made by fuel type, and 3) the inclusion of  
36 emission temporal variations (version 1.7 only indicates annual emission fields). Given  
37 CDIAC estimates have been one of well-respected, widely-used in the carbon research  
38 community (e.g. Ballantyne et al., 2012; Le Quéré et al., 2016), our philosophy in our  
39 emission data development is we develop and deliver an extended, comprehensive global  
40 gridded emission data product, fully utilizing CDIAC emissions data (e.g. emission estimates  
41 in both tabular and gridded forms). We also extend/upgrade CDIAC emission data where  
42 possible. Our emission modeling framework was also designed to produce an emission data  
43 product in a timely manner, with updated information. As our ODIAC data product is based  
44 CDIAC emission data, our emission data production capability is significant given the  
45 expected discontinuity of future CDIAC emission data.

46 Starting with national emission estimates as an input, our model framework achieves  
47 monthly, global FFCO<sub>2</sub> gridded fields via preprocessing, and spatial and temporal  
48 disaggregation. CDIAC national estimates made by fuel type (liquid, gas, solid, cement



1 production, gas flare and international bunker emissions) are further divided into an extended  
2 set of ODIAC emission categories (point source, non-point source, cement production, gas  
3 flare, international aviation and marine bunker (further described in section 3). It is important  
4 to note that ODIAC2016 carries emissions from international bunker (international marine  
5 bunker and aviation, often accounts for few percent of the global total emissions), which are  
6 not included in the CDIAC gridded emission data products (CDIAC gridded emission data  
7 only indicate national emissions and international bunker emissions are often not considered  
8 to be a part of national emissions in an international convention). With the inclusion of  
9 international bunker emissions, we provide more comprehensive global gridded emission  
10 field. We extended CDIAC estimates over the recent years that was not yet covered in the  
11 version of CDIAC estimates (2014-2016), in order to support near-real time CO<sub>2</sub>  
12 simulations/analysis. Emissions are then spatially distributed using a wide variety of spatial  
13 data (e.g. point source geographical location, nighttime light data and flight/ship tracks,  
14 further described in section 4). We adopts emission seasonality from existing emission  
15 inventories for particular emission categories (further described in section 5).

16 In the following sections (section 3-5), we describe how ODIAC2016 was developed. It is  
17 important to note that ODIAC2016 is based on the best available data at the time of the  
18 development (ODIAC2016 was released in September 2016). Thus, some of the emission  
19 estimates and underlying data used in ODIAC2016 might have been outdated. For traceability  
20 purpose, data used in this development, their versions/editions, and data sources are  
21 summarized in Appendix A. Following the results and evaluation section (section 6), we  
22 discuss caveats and current limitations in our modeling framework/emission data product  
23 (section 7), and then describe how we will update ODIAC emission data product with  
24 updated fuel statistics and/or emission information (section 8). Given recent most of  
25 atmospheric CO<sub>2</sub> inversion studies focused on years after 2000, we put a priority to develop  
26 emission data for years after 2000 and deliver to the science community in a timely manner.  
27 Future versions of ODIAC data however might have a longer, extended time coverage.  
28 Currently ODIAC data are provided in two data formats: 1) global 1×1 km (30 arc second)  
29 monthly data in GeoTIFF format (only includes emissions over land) and 2) 1×1 degree  
30 annual (12 month) data in netCDF format (includes international bunker emissions). The  
31 improvements with the use of improved nighttime light data in the 1×1 km data were  
32 documented in Oda et al. (2012). This manuscript thus focuses on the comprehensive global  
33 FFCO<sub>2</sub> fields at a 1×1 degree, otherwise specified.

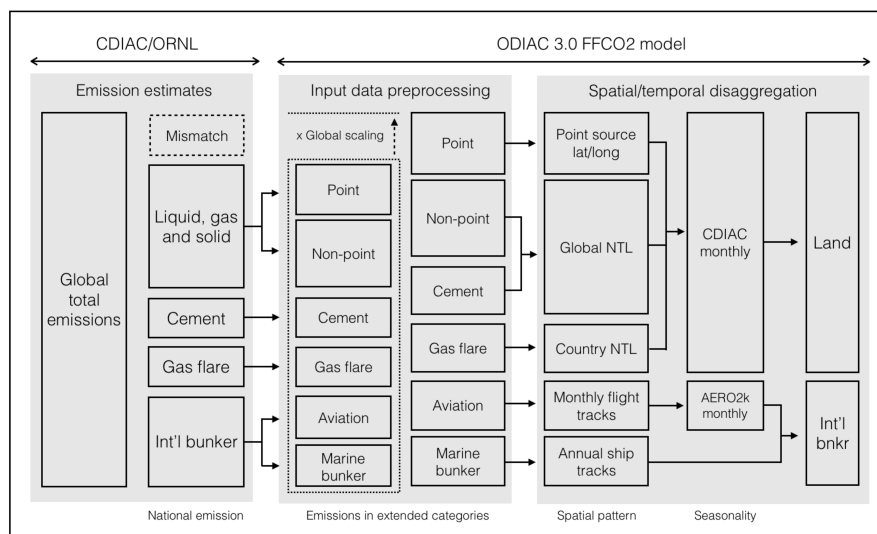


**Figure 1.** A schematic figure of the ODIAC emission modeling framework (defined as “ODAIC 3.0 FFCO2 model”). Starting with CDIAC national emission estimates made by fuel type (emission estimates), the CDIAC emission estimates are first divided into extended ODIAC emission categories (input data processing, see section 3). ODIAC 3.0 FFCO2 model then distributes the emissions in space and time, using point source geolocation information and spatial data depending on emission category such as nighttime light (NTL), and aircraft and ship fleet tracks (spatial disaggregation, see section 4). The emission seasonality for emissions over land and international aviation were adopted from existing emission inventories (temporal disaggregation, see section 5).

1

2

3

### 3. Emission estimates and input emission data preprocessing

4

5

#### 3.1 Emissions for 2000-2013

6

7

CDIAC FFCO2 emissions estimates are based on fuel statistic data published as United Nation Energy Statistics Database (Boden et al., 2017). Emission estimates are calculated on global, national and regional basis and by fuel type in the method described in Marland and Rotty (1984). CDIAC also provides their own gridded emission data products that indicate annual and monthly FFCO2 fields at a  $1 \times 1$  degree (Andres et al., 1996; Andres et al., 2011). ODIAC2016 is primarily based on the year 2016 version of the CDIAC national estimates (Boden et al., 2016), which was the most up-to-date CDIAC emission estimates at the time of the data development (currently Boden et al. 2017 is the latest). We first aggregated the CDIAC national (and regional) emissions estimates to 65 countries and 6 geographical regions (North America, South and Central Americas, Europe and Eurasia, the Middle East, Africa, and Asia Pacific) defined in Oda and Maksyutov (2011) (see the country/region definitions are shown in Table 1 in Oda and Maksyutov 2011). In addition to the national and geographical categories, we decided to include Antarctic fishery emissions, which are from fishery activities over the Antarctic Ocean ( $< 60S$ ,  $1 \sim 4$  kTC/yr over 1987-2007 by Boden et al., 2016), as an individual emission region and distributed in the same way as Andres et al.

21



1 (1996). Emissions from international bunker and aviation are not included in national  
2 emissions by international convention. Thus CDIAC gridded emission data products do not  
3 include the emissions from international bunker and aviation although CDIAC do have  
4 records of those emissions on national/regional basis. ODIAC2016 includes those emissions  
5 to achieve comprehensive global FFCO<sub>2</sub> gridded emission fields.

6 In CDIAC emission estimates, the global total emission and national total emissions are  
7 obtained by different calculation methods (global fuel production vs. apparent national fuel  
8 consumption, see Andres et al., 2012) and the CDIAC national totals do not sum to the  
9 CDIAC global total due to the difference in calculation method and inconsistencies in the  
10 underlying statistical data (e.g. import/export totals) (e.g. Andres et al., 2012). We thus  
11 calculate the difference between the global total and the sum of national totals and scaled up  
12 national totals to account for the difference. Andres et al. (2014) report global total emission  
13 estimates calculated with production data (as opposed to apparent consumption data) have the  
14 smallest uncertainty (approximately 8% (2 sigma)). It is thus used as the reference for global  
15 carbon budget analysis (e.g. Le Quéré et al., 2016). Inversion analysis is an extended version  
16 of the global carbon budget analysis using atmospheric models. We thus believe that  
17 imposing transport models and/or inversion models in a consistent way with the global carbon  
18 budget analysis such as Le Quéré et al. (2016) has significance, although we sacrifice the  
19 accuracy of the national/regional emission estimates. Due to the global scaling, national totals  
20 in ODIAC2016 differ from the estimates originally reported by CDIAC. The differences  
21 between the CDIAC global total and the sum of national emissions are often few percent and  
22 thus the magnitude of the scaling is often within the uncertainty range of national emissions  
23 (e.g. 4.0 to 20.2%, Andres et al., 2014).

24

### 25 3.2 Emissions for 2014-2015

26

27 The year 2016 version of the CDIAC estimates only covers years to 2013 (Boden et al.,  
28 2016). We thus extrapolated the year 2013 CDIAC emissions to years 2014 and 2015 using  
29 the year 2016 version of BP global fuel statistical data (BP, 2017). Our emission extrapolation  
30 approach are the same as Myhre et al. (2009) and Le Quéré et al. (2016). Emissions from  
31 cement production and gas flaring (approximately 5.7% and 0.6% of the 2013 global total,  
32 Boden et al., 2016) were assumed to be as the same as year 2013. International bunker  
33 emissions were scaled using changes in national total emissions.

34

### 35 3.3 CDIAC emission sector to ODIAC emission categories

36

37 CDIAC national emission estimates (prepared by fuel type) were re-categorized to our own  
38 ODIAC emission categories (point source, nonpoint source, cement production, gas flare and  
39 international aviation and international marine bunker). Following Oda and Maksyutov  
40 (2011), the sum of emissions from liquid, gas and solid fuels was further divided into point  
41 source emissions and non-point source emissions. The total emissions from point sources  
42 were estimated using national total power plant emissions calculated using CARMA (Oda and  
43 Maksyutov, 2011). As mentioned earlier, CDIAC gridded emission data products only  
44 indicate national emissions and do not include international bunker emissions (Andres et al.,  
45 1996, Andres et al., 2011). In contrast, EDGAR provides bunker emissions in their gridded  
46 data product (JRC, 2017). Peylin et al. (2013) show some models include international bunker  
47 emissions and some do not, although the difference due to the inclusion/exclusion of the  
48 international bunker emissions in the prescribed emissions could be corrected afterwards





1 (Peylin et al., 2013). In ODIAC2016, we carry CDIAC international bunker emissions  
2 reported on country basis to achieve the complete picture of the global fossil fuel emissions.  
3 Country total bunker emissions (aviation plus marine bunker) were distributed using spatial  
4 proxy data adopted from other emission inventories described later (see section 4.3).  
5 Although CDIAC does not report emissions from international aviation and marine bunker  
6 separately, we loosely estimated those two emissions using U.N. statistics. We estimated the  
7 fraction of aircraft emissions using jet fuel and aviation gasoline consumption and then the  
8 international bunker emissions were divided into aircraft and marine bunker emissions.  
9

10

#### 11 **4. Spatial emission disaggregation**

12

##### 13 4.1 Emissions from point sources, non-point sources and cement production

14

15 We define the sum of the emissions from solid, liquid and gas fuels as land emission (see  
16 Fig. 1). Land emissions are further divided into two emission categories (point source  
17 emissions and non-point source emissions) and then distributed in the ways described in Oda  
18 and Maksyutov (2011): Point source emissions are mapped using power plant profiles  
19 (emission intensity and geographical location) and non-point source emissions are distributed  
20 using nighttime light data collected by the Defense Meteorological Satellite Program (DMSP)  
21 satellites. To avoid a difficulty in emission disaggregation especially over bright regions in  
22 nighttime light data (e.g. cities), Oda and Maksyutov (2011) employed a product that does not  
23 have an instrument saturation issue, rather than regular nightlight product. ODIAC2016  
24 employs the latest version of the special nighttime light product (Ziskin et al., 2010). The  
25 improved nighttime light data has mitigated the underestimation of emissions over dimmer  
26 areas seen in ODIAC v1.7 (Oda et al., 2010). Nighttime light data are currently available for  
27 multiple years (1996-97, 1999, 2000, 2002-03, 2004, 2005-06 and 2010). In ODIAC2016,  
28 due to the lack of information, emissions from cement production were spatially distributed as  
29 a part of non-point source emissions, although those emissions should have been distributed  
30 as point sources. This needs to be fixed in future versions in ODIAC emission data.  
31

32

##### 33 4.2 Emissions from gas flaring

34

35 In the ODIAC v1.7, emissions from gas flaring were not considered (Oda and Maksyutov  
36 2011). Nighttime light pixels corresponding to gas flares often appear very bright and would  
37 result in creating strong point sources in emission data (Oda and Maksyutov, 2011). We thus  
38 identified and excluded those bright gas flare pixels before distributing land emissions, using  
39 another global nighttime light data product that was specifically developed for gas flares by  
40 National Oceanic and Atmosphere Administration (NOAA), National Centers for  
41 Environmental Information (NCEI, former National Geophysical Data Center (NGDC)) (Oda  
42 and Maksyutov, 2011). In ODIAC2016 we separately distributed CDIAC gas flare emissions  
43 using the  $1 \times 1$  km nightlight-based gas flare maps developed for 65 individual countries  
44 (Elvidge et al., 2009). Other than the 65 countries, gas flare emissions were distributed as a  
45 part of land emissions.

46

##### 47 4.3 Emissions from international aviation and marine bunker



1 Emissions from international aviation and marine bunker were distributed using aircraft and  
2 ship fleet tracks. International aviation emissions were distributed using the AERO2k  
3 inventory (Eyers et al., 2005). The AERO2k inventory was developed by a team at  
4 Manchester Metropolitan University (MMU) and indicates fuel use and NO<sub>x</sub>, CO<sub>2</sub>, CO,  
5 hydrocarbon and particulate emissions for 2002 and 2025 (projected) with injection height at  
6 a 1 × 1 degree spatial resolution on monthly basis. We used their column total CO<sub>2</sub> emissions  
7 to distribute emissions to a single layer. International marine bunker emissions were  
8 distributed at a 0.1 × 0.1 degree using an international marine bunker emission map from the  
9 EDGAR v4.1(JRC, 2017). We decided not to adopt an international and domestic shipping  
10 (1A3d) map from the EDGAR v4.2 as it includes domestic shipping emissions that we does  
11 not distinguish.

12  
13

#### 14 **5. Temporal emission disaggregation**

15

16 The inclusion of the temporal variations is often a key in transport model simulation. For  
17 CO<sub>2</sub> flux inversion, the potential biases in flux inverse emission estimates due to the lack of  
18 temporal profiles was suggested by Gurney et al. (2005). In ODIAC2016, we adopt the  
19 seasonal emission changes developed by Andres et al. (2011). The CDIAC monthly gridded  
20 data include monthly national emissions gridded at a 1 × 1 degree resolution (Andres et al.  
21 2011). We normalized the monthly emission fields by the annual total and the applied to our  
22 annual emissions over land. The seasonality in ODIAC2016 is based on the year 2013 version  
23 of the CDIAC monthly gridded emission. The CDIAC monthly emission data do not cover  
24 the recent years. For recent years, we created a climatological seasonality using monthly  
25 CDIAC data from 2000-2010 (excepting 2009 where economic recession happened). Due to  
26 the limited availability of monthly fuel statistical data, Andres et al. (2011) used proxy  
27 country and also seasonality allocated by Monte Carlo simulations. The years between 2000-  
28 2010 were most data rich period and mostly explained by data (see Fig. 1 in Andres et al.,  
29 2011).

30 Although ODIAC2016 only provides monthly emission fields, users can derive hourly  
31 emissions by applying scaling factors developed by Nassar et al. (2013). The Temporal  
32 Improvements for Modeling Emissions by Scaling (TIMES) is a set of scaling factors which  
33 one can derive weekly emissions and diurnal emissions from any monthly emission data that  
34 you use. Temporal profiles are collected from Vulcan, EDGAR and best available  
35 information and gridded on a 0.25 × 0.25 degree (Nassar et al., 2013). TIMES also includes  
36 per capita emissions corrections for Canada (Nassar et al., 2013).

37  
38



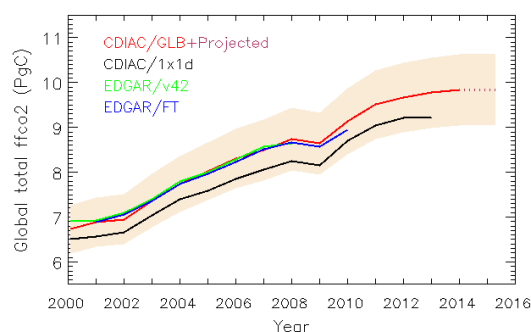


**Figure 2.** Global emission time series from four gridded emission data: CDIAC (red, 2000-2013) plus projected emissions (dashed maroon, 2014-2015) (values taken from ODIAC), CDIAC 1×1 degree (black, 2000-2013), EDGAR v4.2 (green, 2000-2008) and EDGAR v4.2 Fast Track (blue, 2000-2010). The values here are given in the unit of peta gram (= giga tonnes) carbon per year. The shaded area indicated in tan is a two-sigma uncertainty range (8%) estimated for CDIAC global total emission estimates by Andres et al. (2014).

1

2

3

## 6. Results and discussions

4

5

### 6.1 Annual global emissions

6

7 In Fig. 2, global emission time series from different emission data were compared to give an  
8 idea of agreement among them. We calculated the global total for each year from four gridded  
9 emission data for the period of 2000-2016: CDIAC global total + projection (taken from  
10 ODIAC2016), CDIAC gridded data (hence, no international bunker emissions), two versions  
11 of EDGAR gridded data (v4.2 and FastTrack). The uncertainty range (shaded in tan) is 8% (2  
12 sigma) estimated for CDIAC global by Andres et al. (2014). Those gridded emission data are  
13 often used in global atmospheric CO<sub>2</sub> inversion analysis (e.g. Peylin et al., 2013). To account  
14 for the difference in emission reporting categories (e.g. fuel basis in CDIAC vs. emission  
15 sector basis in EDGAR), the EDGAR totals were calculated as the “total short cycle C”  
16 emissions minus the sum of emissions from agriculture (IPCC code: 4C and 4D), land use  
17 change and forestry (5A, C, D, F and 4E) and waste (6C) (see more details on emission  
18 sectors documented in JRC (2017)). International aviation (1A3a) and navigation (1A3b)  
19 were thus included in values for EDGAR time series. The authors acknowledge the JRC has  
20 updated EDGAR emission time series for 1970-2012 in November 2014 (JRC, 2017). This  
21 study however uses gridded emission data, which are not fully based on the updated emission  
22 estimates, in order to characterize differences from gridded emission data, especially for  
23 potential data users in the modeling community.

24 All four global total values obtained from four gridded emission data agree well within 8%  
25 uncertainty. The difference between ODIAC and CDIAC (3.3%-5.7%) were largely  
26 attributable to the international bunker emissions and global correction. ODIAC (where the  
27 total was scaled by CDIAC global total) and two versions EDGAR showed minor differences  
28 in magnitude (0.3%-2.7%) and trend, which are largely attributable to the differences in the



1 underlying statistical data (e.g. U.N. Stat vs. EIA from different inventory years) and the  
2 emission calculation method (fuel basis vs. sector basis). Global total estimates at 5-year  
3 increments are shown in Table 1. For the year 2014 and 2015, we estimated the global total  
4 emissions 9.836 and 9.844 PgC. Boden et al. (2017) reported the latest estimate for year 2014  
5 global total emission as 9.855 PgC. Our projected 2014 emission estimate was lower than the  
6 latest estimate by approximately 0.02 PgC (0.2%).

7  
8  
9 **Table 1.** Global total emission estimates for year 2000, 2005 and 2010 from four gridded  
10 emission data (ODIAC2016, CDIAC, EDGAR v4.2 and EDGAR FastTrack). Values for two  
11 versions of EDGAR emission data were calculated by subtracting emissions from agriculture  
12 (IPCC code: 4C and 4D), land use change and forestry (5A, C, D, F and 4E) and waste (6C)  
13 from the total EDGAR CO<sub>2</sub> emissions (total short cycle C).

14

Year	ODIAC2016	CDIAC national	EDGAR v4.2	EDGAR FT
2000	6727	6506 (-3.3%)	6907 (+2.7%)	N/A
2005	8025	7592 (-5.4%)	8005 (-0.2%)	7959 (-0.8%)
2010	9137	8694 (-4.8%)	N/A	8950 (-2.0%)

15

16

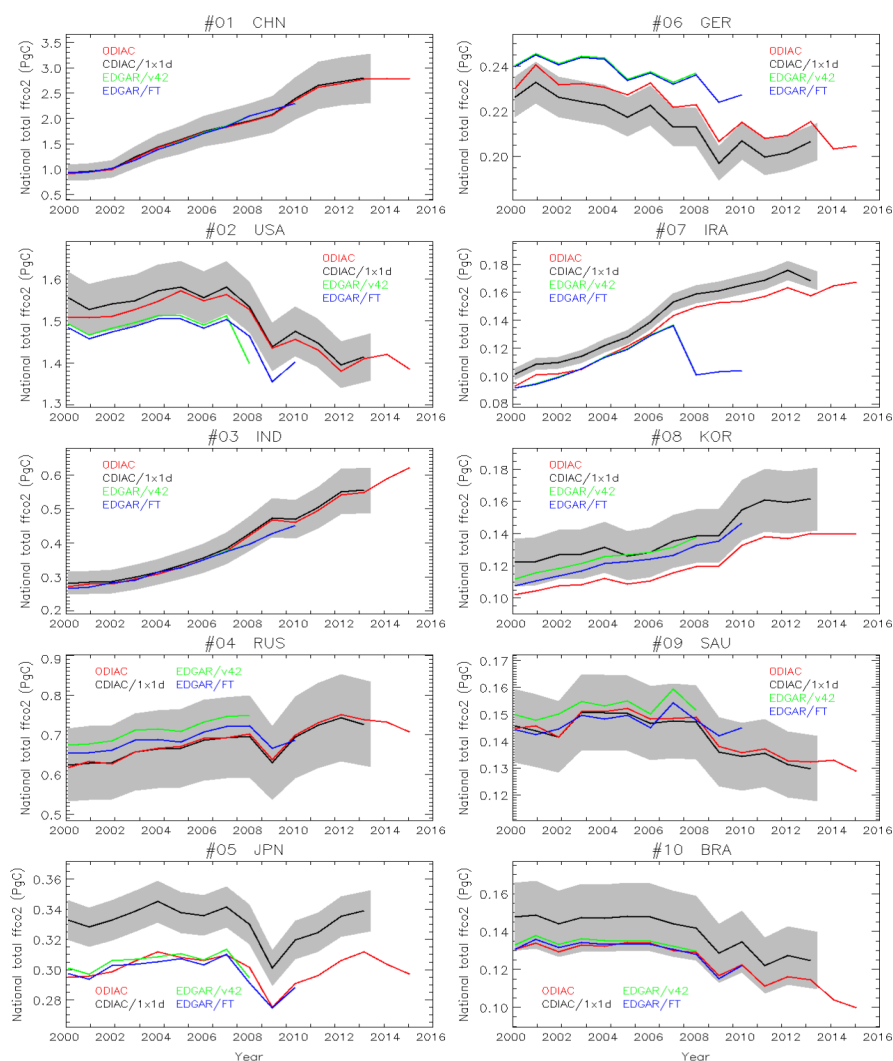


**Figure 3.** National emission time series for top 20 emitting countries (China, U.S., India, Russian Federation, Japan, Germany, Islamic Republic of Iran, Republic of Korea (South Korea), Saudi Arabia and Brazil). The values are given in the unit of peta gram (=giga tonnes) carbon per year. The values are calculated using gridded emission data, not tabular emission data. The national total values in the plots might be thus different from values indicated in the tabular form due to the emission disaggregation. The shaded area in grey indicates a two-sigma uncertainty range estimated by Andres et al. (2014) (see Table 2).

1

2

3

4

5

6

Fig. 3 shows the same type of comparison as Fig. 2, but for the top 10 emitting countries (China, US, India, Russian Federation, Japan, Germany, Islamic Republic of Iran, Republic of Korea (South Korea), Saudi Arabia and Brazil, according to the year 2013 ranking reported by CDIAC). We aggregated all the four gridded emission fields to a common  $1 \times 1$  degree field



1 and sampled using the 1×1 degree country mask used in CDIAC emission data development.  
 2 The annual uncertainty estimates for national total emissions (2 sigma) are made following  
 3 the method described by Andres *et al.*, (2014) and values are shown in Table 2. In the  
 4 analysis presented in Fig. 3, emissions from international aviation (1A3a) and navigation  
 5 (1A3b) are excluded. All four national total values sampled from four gridded emission data  
 6 at a 1×1 degree often agree within the uncertainty estimated by Andres *et al.* (2014).  
 7 Systematic differences of ODIAC from CDIAC can be largely explained by 1) global  
 8 correction (the total was scaled using CDIAC global total) and 2) the differences in emissions  
 9 disaggregation methods. Although ODIAC is expected to indicate slightly higher values than  
 10 CDIAC (often few percent) because of the global correction (note global correction can be  
 11 negative, despite of the depiction in Fig. 1), ODIAC sometimes indicates values lower than  
 12 CDIAC more than few percent (see Japan in Fig. 3 as an example). This is due to a sampling  
 13 error using the 1×1 degree country map in the analysis. The aggregated 1×1 degree ODIAC  
 14 field is slightly larger than that of CDIAC especially because of the coastal areas depicted a  
 15 high-resolution in the original 1×1 km emission field. This type of sampling error was  
 16 discussed in Zhang *et al.* (2014). ODIAC employs a 1×1 km coastline and a 5×5 km country  
 17 mask as described in Oda and Maksyutov (2011). Thus, the use of 1×1 degree CDIAC  
 18 country map results in missing some land mass (hence, CO<sub>2</sub> emissions). Similar sampling  
 19 error can happen for countries that are physical small and island countries, depending on the  
 20 resolution of analysis. Despite of the sampling error, the authors used the CDIAC 1×1 degree  
 21 country map to do this comparison analysis with having CDIAC as a reference. The lower  
 22 emission indicated by ODIAC or EDGAR in this analysis does not always mean the national  
 23 total emissions are lower. The emission estimates at national level often agree well even  
 24 among different emission inventories (e.g. Andres *et al.*, 2012).

25

26

27 **Table 2.** Annual uncertainty estimates associated with CDIAC national emission estimates.28 The uncertainty estimates were made following the method described by Andres *et al.* (2014).29 The national total emissions for the year 2013 were taken from Boden *et al.* (2016).

30

Ranking #	Country	2013 emissions in kTC (% of the global total)	Uncertainty (%)
1	China	2,795,054 (28.6%)	17.5
2	U.S.	1,414,281 (14.5%)	4.0
3	India	554,882 (5.7%)	12.1
4	Russia Federation	487,885 (5.0%)	14.8
5	Japan	339,074 (3.5%)	4.0
6	Germany	206,521 (2.1%)	4.0
7	Islamic Republic of Iran	168,251 (1.7%)	9.4
8	Republic of Korea	161,576 (1.7%)	12.1
9	Saudi Arabia	147,649 (1.5%)	9.4
10	Brazil	137,354 (1.4%)	12.1

31

32

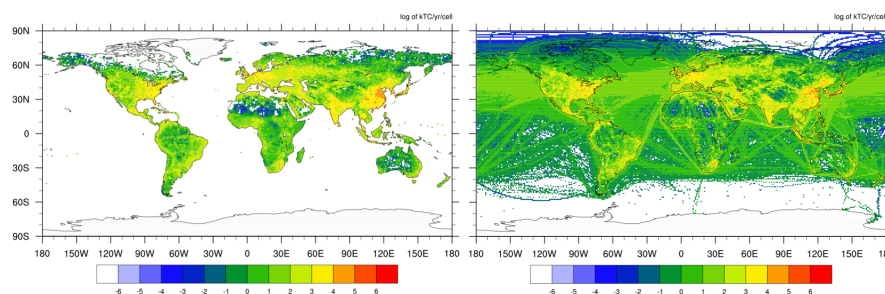


**Figure 4.** Year 2013 global fossil fuel CO<sub>2</sub> emissions distributions from CDIAC (left, 8.36 PgC) and ODIAC (right, 9.78 PgC). The ODIAC emission field was aggregated to a common 1 × 1 degree resolution. The value is given in the unit of log of thousand tonnes C/cell.

1  
2  
3  
4  
5  
6  
7  
8  
9  
10  
11  
12  
13  
14  
15  
16  
17  
18

## 6.2 Global emission spatial distributions

The global total emission fields of CDIAC gridded emission data and ODIAC2016 for the year 2013 (the most recent year CDIAC indicates) are shown in Fig. 4. Emission fields are shown at a common 1×1 degree. The major difference seen between two fields is primarily due to inclusion/exclusion of emissions from international bunker emissions that largely account for the differences indicated in Table 1. A breakdown of ODIAC year 2013 emission field are presented by emission category in Fig. 5. Emission fields for point sources, non-point sources, cement production and gas flaring were produced at a 1×1 km resolution in ODIAC 3.0 model, but as mentioned earlier, we focus on the 1×1 degree version of ODIAC2016 in this manuscript. In CDIAC gridded emission data, those emissions are distributed by population data without fuel type distinction. In ODIAC 3.0 model, we have added additional layers of consideration in the emission modeling from the conventional CDIAC model and add the possibility of future improvement with improved emission proxy data.

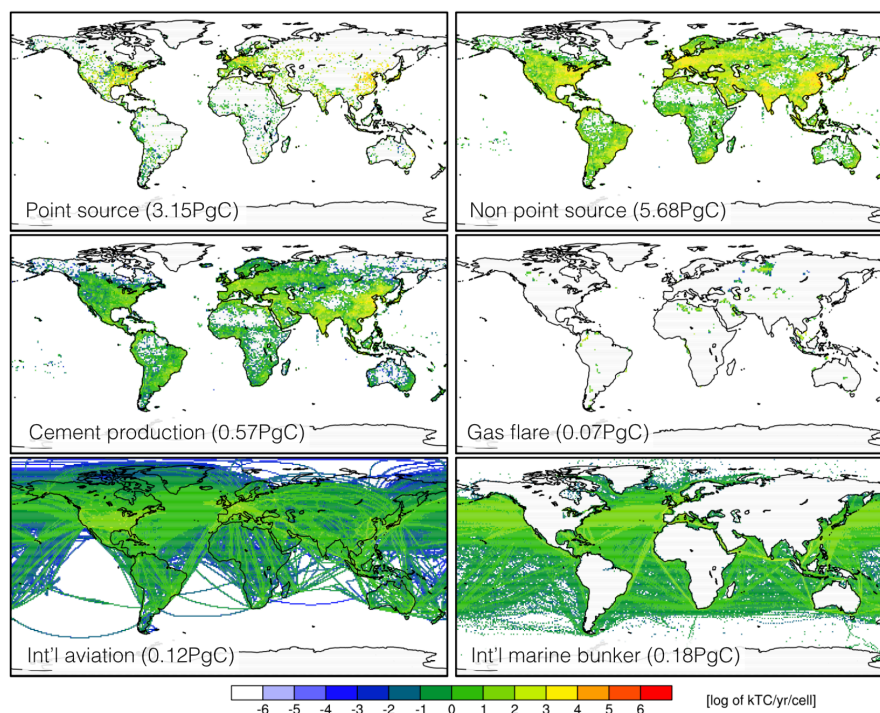


**Figure 5.** Year 2013 global distributions of ODIAC fossil fuel emissions by emission type. The panels show emissions from (from top to the right, then down) point source, non-point source, cement production, gas flaring, international aviation and international shipping. The values in the figures are given in the unit of log of thousand tonnes carbon/year/cell ( $1 \times 1$  degree). The numbers in the brackets are the total for the category emissions in the unit of PgC (total year 2013 emission in ODIAC2016 was 9.78 PgC).

1  
2  
3 In Fig. 6, we compared the four global gridded products over land and also calculated  
4 differences from ODIAC2016 (shown in Fig. 7). It is often very challenging to evaluate the  
5 accuracy and uncertainty of gridded emission data, because of the lack of direct physical  
6 measurements at grid scales (Andres et al., 2016). Recent studies have attempted to evaluate  
7 the uncertainty of gridded emission data by comparing emission data each other (e.g. Oda et  
8 al., 2015; Hutchins et al., 2016). The differences among emission were used as a proxy for  
9 uncertainty. However, it is important note that such evaluation does not give us an objective  
10 measure of which one is closer to truth, beyond characterizing the differences in emission  
11 spatial patterns and magnitudes from methodological viewpoints (e.g. emission estimation  
12 and disaggregation). Some of the gridded emission data are partially disaggregated using  
13 commercial information, which users are often not authorized to fully disclose the  
14 information used and thus makes the comparison even less meaningful and/or significant.  
15 Oda et al. (2015) also discussed that emission inter-comparison approaches often do not allow  
16 us to evaluate two distinct uncertainty sources (emissions and disaggregation) separately. In  
17 addition, because of the use of emission proxy for emission disaggregation (rather than  
18 mechanistic modeling), such comparison can be only implemented at an aggregated, coarse  
19 spatial resolution. These issues will be further discussed in the Section 7.



1 Because of the limitation mentioned above, we here compared emission data only to  
2 characterize the differences that can be explained by the differences in emission  
3 disaggregation methods. We implemented this comparison exercise using 2008 emission field  
4 aggregated at a  $1 \times 1$  degree resolution. Year 2008 is the most recent year where all the four  
5 emission fields are available. The major emission spatial patterns (e.g. emitting regions such  
6 as North America, Europe and East Asia) are overall very similar as the correlations were  
7 driven by national emission estimates (which we already saw good agreement earlier), but we  
8 do see differences due to emission disaggregation at subnational scale. Because of the use of  
9 nightlight, ODIAC did not indicate emissions over some of the areas (e.g. Africa and Eurasia)  
10 while others do. Especially, EDGAR has emissions over those areas that are largely explained  
11 by line source emissions such as transportation. Overall, ODIAC tends to put more emissions  
12 towards populated areas than suburbs. This is also explained by the lack of line sources. In  
13 EDGAR v4.2, domestic fishery emissions can be seen, but not in EDGAR FT. Even in these  
14 two EDGAR versions, we can confirm the subnational differences at United States, Europe  
15 and China.  
16  
17

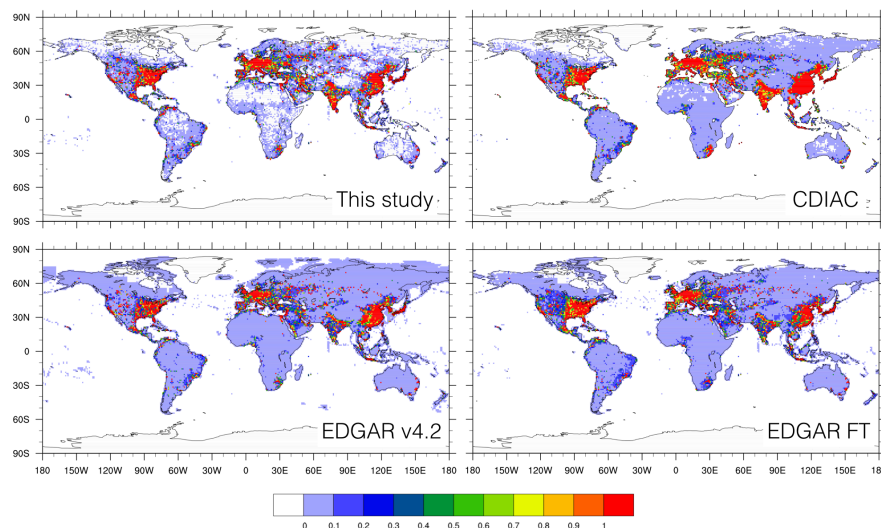


**Figure 6.** Land emissions from ODIAC (upper left), CDIAC (upper right), two versions of EDGAR emission data (v4.2 lower left and v4.2 Fast Track lower right). The units are tonnes carbon/year/ cell ( $1 \times 1$  degree). In addition to excluding emissions from international aviation and marine bunker, some of the sector emissions were subtracted from EDGAR short cycle total emissions to account for the differences in emission calculation methods between CDIAC and EDGAR, as also done earlier. The emission fields for the year 2008 were used.

18



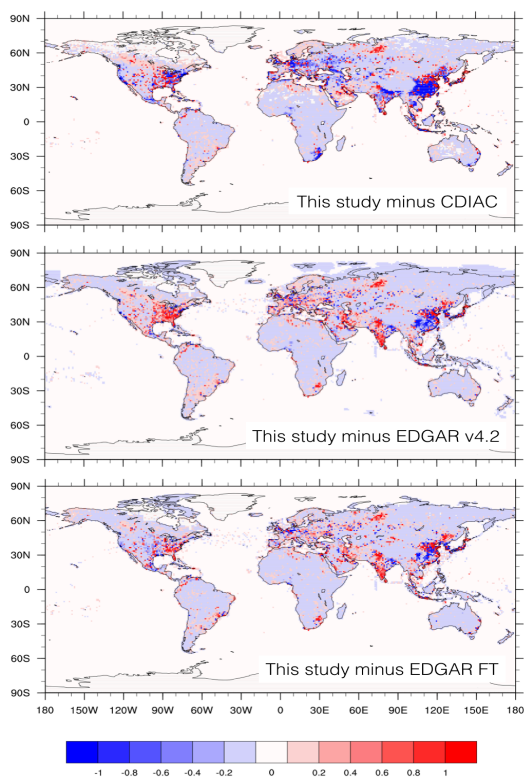


**Figure 7.** ODIAC-other emission data differences. CDIAC (upper right), two versions of EDGAR (v4.2 lower left and v4.2 Fast Track lower right). The units are tonnes carbon/year/cell ( $1 \times 1$  degree). Note that the differences are defined as ODIAC (this study) minus others.

1  
2  
3  
4  
5  
6  
7  
8  
9  
10  
11

### 6.3 Regional emission time series.

Fig. 8 shows time series of regional fossil fuel emissions aggregated over 11 land regions defined in the TransCom transport model intercomparison experiment (e.g. Gurney et al., 2002). The global seasonal variation and the associated uncertainty have been presented and discussed in Andres et al. (2011). Here monthly total emission values were calculated for eleven TransCom land regions and presented with the associated uncertainty values (see Table 3). The monthly total values were calculated in both excluding international bunker emissions (hence, land emissions only) and including the emissions. The uncertainty range



1 was calculated by mass weighted uncertainty estimates of countries that fall into the regions.  
2 The uncertainty ranges shown in Fig. 8 are annual uncertainty plus the monthly profile  
3 uncertainty (12.8%, reported by Andres et al., 2011). Monthly time series are presented for  
4 land only emissions and land and international bunker emission (here, largely aviation  
5 emissions). As described earlier, the emission seasonality was adopted from Andres et al.  
6 (2011). The patterns in emission seasonality are often largely characterized by the large  
7 emitting countries within the regions (e.g. U.S. for region 2; China for region 8). Since  
8 Andres et al. (2011) used geographical closeness (also, type of economic systems) to define  
9 proxy countries, the countries in the same TransCom regions can have similar or the same  
10 seasonal patterns in their emissions.

11 As we can see in Fig. 4 (panel plot for aviation emissions), aviation emissions are intense  
12 over North America, Europe and Asia. Global total aviation emission was approximately 0.12  
13 PgC/yr in 2013 and it often does not account for a large portion of the global total (1.2% of  
14 the global total in 2013). However, considering the fact that those emissions are concentrated  
15 in particular areas such as North America, Europe and East Asia, rather than evenly  
16 distributed in space, and often imposed at the surface layer in transport model simulation, care  
17 must be taken to achieve an accurate atmospheric CO<sub>2</sub> transport model simulations (Nassar et  
18 al., 2010). Aviation emissions were often around 0.5-5.1% of the land total emissions over the  
19 most regions, but as large as 12.7% (North American Boreal).

20

21

## 22 **7. Current limitations, caveats and future prospects**

23

24 As ODIAC emission data product is now used for a wide variety of carbon cycle research  
25 (e.g. global, regional inversions, urban emission studies), it would be useful to note/discuss  
26 issues/limitations and caveats in our emission data as well as modeling framework. Some of  
27 the issues/limitations are specific to our study, however the majority of them are often shared  
28 by existing other gridded emission data and or emission models.

29

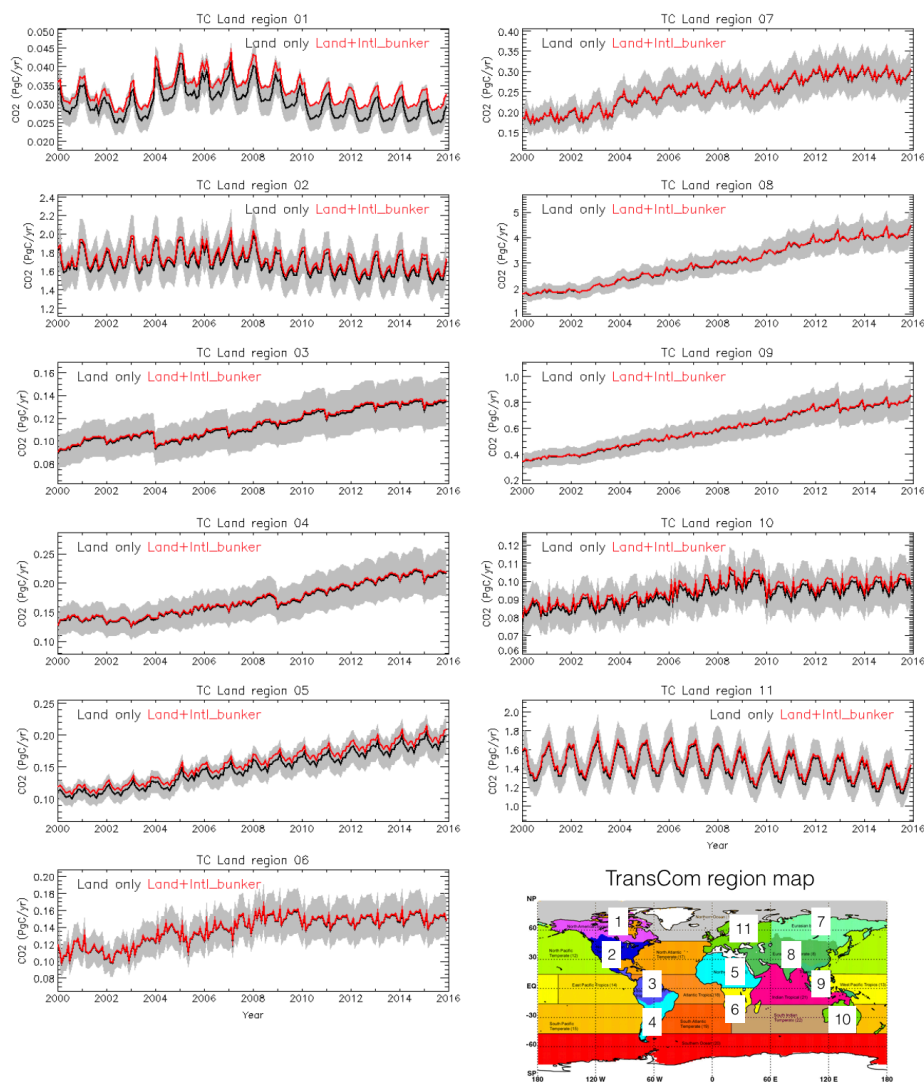


**Figure 8.** Emission time series over inversion analysis land regions defined by the Transport model intercomparison (TransCom) project (Gurney *et al.*, 2002). The TransCom region map (bottom right) is available from [http://transcom.project.asu.edu/transcom03\\_protocol\\_basisMap.php](http://transcom.project.asu.edu/transcom03_protocol_basisMap.php) (last access: 8 November, 2016). Black lines indicate ODIAC  $1 \times 1$  degree monthly emissions. The monthly emissions are calculated using  $1 \times 1$  degree ODIAC emission data. The uncertainty range was calculated by mass weighted uncertainty estimates of countries that fall into the regions (see Table 3). The uncertainty ranges shown in Fig. 8 are annual uncertainty plus the monthly profile uncertainty (12.8%, reported by Andres *et al.*, 2011). Note scales in the vertical axis are different.

1  
2

1  
2  
3  
4  
5  
6  
7  
8

**Table 3.** Annual total emission over TransCom land regions and the associated uncertainty estimates. The total emissions were calculated using ODIAD2016 gridded emission data. The numbers in the bracket are values including international bunker emissions. The uncertainty estimates were mass weighted values of uncertainty estimates of countries that fall in the regions. Country uncertainty estimates were estimated using the method described Andres et al. (2014). The values were reported as 2-sigma uncertainty.

Region #	Region name	Uncertainty (%)
1	North American Boreal	3.7
2	North American Temperate	3.7
3	South American Tropical	9.6
4	South American Temperate	12.8
5	Northern Africa	5.1
6	Southern Africa	10.6
7	Eurasian Boreal	12.4
8	Eurasian Temperate	7.8
9	Tropical Asia	11.8
10	Australia	4.0
11	Europe	3.8

9  
10  
11  
12  
13  
14  
15  
16  
17  
18  
19  
20  
21  
22  
23  
24  
25  
26  
27  
28  
29  
30  
31  
32  
33

## 7.1 Emission estimates

In the production of ODIAC2016, we used several versions/editions of CDIAC estimates (e.g. global estimates, national estimates and monthly gridded data). This could often happen in emission data production, as some of the underlying data are not updated/upgraded at the time of emission data production (we often start updating emission data after new fuel statistical data are released). We sometimes accept the inconsistency and try to use the most up-to-date information available. For example, we could use GCP's estimates (e.g. Le Quéré et al., 2016) to constrain the global totals, if CDIAC global total emission estimates are not available. The way we obtained emission estimates for each version is often described in netCDF header information of the emission data product. The use of CARMA power plant estimates for estimating magnitude of point source portion of emissions is hard to eliminate, although ideally this is done using emission estimates that are fully compatible to CDIAC estimates. We are currently examining U.N. statistical data (which CDIAC emission estimates are based on) to assess the ability of explaining power plant emissions.

## 7.2 Emission spatial distributions

### 7.2.1 Point source emissions

Although the use of the power plant geolocation allowed us to achieve improved high-resolution emission spatial distributions over land (Oda and Maksyutov, 2011), the



1 availability of power plant data is often very limited. For example, CARMA does not provide  
2 power plant emissions and its status (e.g. commission/decommission) every year and  
3 furthermore update/upgrade after their version 3.0 database (which dated 2012). The error in  
4 their power plant geolocation is another issue that has been identified (e.g. Oda and  
5 Maksyutov, 2011; Woodard et al., 2015). In ODIAC, the base year emissions (2007) were  
6 projected and all the power plants were assumed to be active over the period (Oda and  
7 Maksyutov, 2011). There are only few global projects that are collecting power plant  
8 information such as the Global Energy Observatory (GEO,  
9 <http://globalenergyobservatory.org/>) and those can be a useful source of data to improve and  
10 supplement CARMA database. Regionally, CARMA can be evaluated using an inventory  
11 such as the U.S. Emissions and Generation Resource Integrated Database (eGRID) (EPA,  
12 2017). However, it is often difficult to find such a well-constructed and documented  
13 inventory for countries that are actually driving the uncertainty in global emissions (e.g.  
14 China and India).

15 Emissions from cement production (which are currently distributed using nightlight by  
16 Ziskin et al., 2010) and gas flare (which is distributed using gas flare nightlight data by  
17 Elvidge et al., 2009) should be distributed as point sources. For gas flare emissions, we are  
18 examining the use of Nightfire (Elvidge et al., 2013a) to pinpoint active gas flares in timely  
19 manner and improve their emissions spatial disaggregation over the recent years.

#### 20 21 7.2.2 Non-point source emissions

22  
23 Nighttime light data has been an excellent proxy for human settlements (hence, CO<sub>2</sub>  
24 emissions) even at a high spatial resolution, however there are some issues to be discussed.  
25 As mentioned earlier, we used an improved version of calibrated radiance data developed by  
26 Ziskin et al. (2010), but those data are only available to seven data periods over the course of  
27 DMSP years (1992-2013). As we do not believe linearly interpolating the existing nightlight  
28 data over the intervening years is necessarily the best way (as done in Asefi-Najafabady et al.,  
29 2014), the same nightlight data has been used for some periods and thus emission  
30 distributions remain unchanged. We are now examining the use of nightlight data collected  
31 from the Visible Infrared Imaging Radiometer Suite (VIIRS) on Suomi National Polar-  
32 orbiting Partnership satellite (e.g. Elvidge et al., 2013b; Román and Stokes, 2015). VIIRS  
33 instruments do not have several critical issues that the DMSP instrument had (e.g. spatial  
34 resolution, dynamic range, quantization and calibration) (Elvidge et al., 2013b). The fully  
35 calibrated nightlight data can be used to map emission changes in space in timely and  
36 consistent manner.

37 In ODIAC, the disaggregation of non-point emissions is solely done using nighttime light  
38 data for estimating subnational emission spatial distribution and no additional subnational  
39 constrain were applied. Rayner et al. (2010) proposed to better constrain subnational emission  
40 spatial distribution by combining population data, nighttime lights and GDP in their Fossil  
41 Fuel Data Assimilation System (FFDAS) framework. Asefi-Najafabady et al. (2014) further  
42 introduced the use of point source information in their disaggregation, the optimization in  
43 their current framework is however under-constrained by the lack of GDP information.  
44 Without having such optimization, the state level per capita emission estimates can provide  
45 subnational constraints. Nassar et al. (2013) evaluated the per capita emissions in CDIAC and  
46 ODIAC emission data over Canada using the national inventory and found that ODIAC  
47 outperformed. However, as the nightlight-population relationship might have a bias for  
48 developing and the least developed countries (Raupach et al., 2010), we would expect we see



1 significant biases over those countries and the per capita estimates can provide a useful  
2 constraint.  
3 As seen in the comparison to other emission data, the major difference from EDGAR  
4 emission spatial distribution was due to the lack of line sources in ODIAC. We do not believe  
5 the result from the emission data comparison can falsify the emission distribution in ODIAC,  
6 as discussed earlier. However, we do expect an inclusion of the line sources would improve  
7 the spatial distributions and emission representations in both cities and rural areas. We are  
8 currently examining the inclusion of transportation network data (e.g. OpenStreetMap) as  
9 proxy for line source emissions to explore the better spatial emission aggregation method.  
10 Oda et al. (2017) recently implemented the idea of adding a spatial proxy for line sources and  
11 improved emission estimates for a U.S. city.

### 12 13 7.2.3. Aviation emissions

14  
15 We estimated emissions from international aviation from CDIAC using U.N. statistical data.  
16 The emissions are currently provided as a single layer emission field, although it is not  
17 appropriate given the nature of the aviation emissions. Nassar et al. (2010) discussed that the  
18 importance of the three dimensional (e.g. x,y,z) emissions for interpreting CO<sub>2</sub> profile. In  
19 current modeling framework, although we maintain the aviation emission injection height  
20 from AERO2k (reduced to 1km interval), we distribute the emissions to a single layer. As  
21 pointed out by Olsen et al. (2013), AERO2k does not agree with other inventories in height  
22 distribution. With noting the caution, we will examine the use of height information from  
23 AERO2k and other data available to us and do sensitivity analysis using transport model  
24 simulations.

### 25 26 27 7.3 Emission temporal profiles.

28  
29 The emission seasonality in ODIAC2016 is based on Andres et al. (2011) and it can be  
30 further extended using the TIMES scaling parameter to hourly scale. We note that the  
31 emission seasonality was based on top 20 emitting countries' fuel statistics and Monte Carlo  
32 simulation (Andres et al., 2011). The emission seasonality for countries other than the top 20  
33 could be less robust. Also, because of the use of Monte Carlo, the seasonality is different over  
34 different editions of monthly emission data. Andres et al. (2011) estimated the monthly  
35 uncertainty as an additional 12.8% (two sigma) over the annual uncertainty. As we often  
36 impose fossil fuel emissions, care must be taken when applied to inversions. Ultimately, as  
37 done by Vogel et al. (2013), we might be able to evaluate temporal profiles from statistical  
38 data and improve them (but only to limited small locations).

### 39 40 7.4 Uncertainties associated with gridded emission fields

41  
42 As mentioned earlier, the evaluation of gridded emission data is often very challenging and  
43 most of the emission data study share this difficulty. Although the emission estimates are  
44 made at global and national scales with small uncertainty (e.g. 8% for global by Andres *et al.*,  
45 2014), considerable errors seem to be introduced when disaggregated (e.g. Hogue et al., 2016;  
46 Andres et al., 2016). Andres et al. (2016) for example estimated the uncertainty associated  
47 with CDIAC gridded emission data on a per grid cell basis with an average of 120% and a  
48 range of 4.0 to 190% (2 sigma). Hogue et al. (2016) closely looked at CDIAC gridded



1 emission data over the U. S. domain and estimated the uncertainty associated with the  $1 \times 1$   
2 degree emission grids as  $\pm 150\%$ . Those errors seem to be unique to the disaggregation  
3 method (Andres et al., 2016). Future funding may allow us to pursue a full uncertainty  
4 analysis of the ODIAC emission data/model, akin to the Andres et al. (2016) approach but  
5 accounting for the greater than one carbon distribution mechanisms utilized in ODIAC  
6 emission modeling framework. All of the spatially distributed gridded emission data  
7 mentioned in this manuscript suffer from the same basic defect: they use proxies to spatially  
8 distribute emissions rather than actual measurements. In addition, evaluating emission  
9 distributions based on nightlight proxy can be challenging as the connection between  $\text{CO}_2$   
10 emissions and proxy is less direct compared to population (e.g. per capita emissions). A  
11 combined use of emission proxy and geolocation data (e.g. power plant location) would also  
12 add additional difficulties to give a comprehensive measure of the uncertainty because of  
13 different type of error/uncertainty sources (e.g. Woodard et al., 2015). As finer spatial scales  
14 are approached, the defect of the proxy approach becomes more apparent: proxies only  
15 estimate emission fields. ODIAC data product has been used not only for global simulations  
16 at an aggregated spatial resolution, but also at very high spatial resolution (e.g. Ganshin et al.  
17 2010; Oda et al. 2012; Lauvaux et al. 2016; Oda et al. 2017). Thus, emission evaluation at a  
18 high resolution has become an important task. One approach we could take for evaluating  
19 high-resolution emission fields is comparing to a local fine-grained emission data product  
20 such as Gurney et al. (2012), acknowledging the limitations of the approach discussed earlier.  
21 Another approach would be evaluating emission data in concentration space, rather than  
22 emission space. As reported in Vogel et al. (2013) and Lauvaux et al. (2016), with  
23 radiocarbon measurements and/or good, spatially dense  $\text{CO}_2$  measurements, a high-resolution  
24 transport model simulation can provide an objective measure for emission data evaluation  
25 (e.g. model-observation mismatch and emission inverse estimate).

26 While the quality (i.e. bias and uncertainty) of the gridded emission estimates remains  
27 unquantified for most of the emission data mentioned in this manuscript, the emission data  
28 are still used because sufficient measurements in space and time are not presently available to  
29 offer a better alternative. At very least, we presented uncertainty estimates over the  
30 aggregated TransCom land regions. We believe that the regional uncertainty estimates are  
31 highly useful for atmospheric  $\text{CO}_2$  inversion modelers, more than uncertainty estimates at a  
32 grid level, which still do not seem to be ready for use. Inversion studies often aggregate flux  
33 estimates over the TransCom land regions to interpret regional carbon budgets, while flux  
34 estimations in their models are done at much higher spatial resolutions (e.g. Feng et al., 2009;  
35 Chevallier et al., 2010; Basu et al., 2013). Taking an advantage of being based on CDIAC  
36 estimates, we adopted the updated uncertainty estimates reported by Andres et al. (2016) and  
37 obtained the regional uncertainty estimates. Those estimates are new and readily usable to the  
38 inversion studies especially when interpreting the regional estimates.

39  
40

#### 41 **8. Product distribution, data policy and future update**

42 ODIAC2016 data product is available from a website hosted by the Center for Global  
43 Environmental Research (CGER), Japanese National Institute for Environmental Studies  
44 (NIES) (<http://db.cger.nies.go.jp/dataset/ODIAC/>, doi: [10.17595/20170411.001](https://doi.org/10.17595/20170411.001)). The data  
45 product is distributed under Creative Commons Attribution 4.0 International (CC-BY 4.0,  
46 <https://creativecommons.org/licenses/by/4.0/deed.en>). ODIAC2016 emission data are  
47 provided in two file formats: 1) global  $1 \times 1$  km (30 arc second) monthly file in GeoTIFF  
48 format (only includes emissions over land) and 2)  $1 \times 1$  degree annual (12 month) file in  
49 netCDF format (includes international bunker emissions). A single, global 1km monthly





1 GeoTIFF file is about 3.7 GB (compressed to 120 MB). The 1 degree netCDF annual file is  
2 about 6MB.

3 We update the emission data on annual basis, following a release of an updated global fuel  
4 statistical data. Future versions of the emissions data are in principle based on updated  
5 version/edition of the underlying statistical data with the same name convention  
6 (ODIACYYYY, YYYY= the release year, the end year is YYYY minus 1). Currently we are  
7 working on the year 2017 version of ODIAC data (ODIAC2017) which covers 2000-2016.  
8 We primarily focus on years after 2000. Future versions of ODIAC data however might have  
9 a longer, extended time coverage.

10

11

## 12 9. Summary

13

14 This manuscript described the year 2016 version of ODIAC emission data (ODIAC2016)  
15 and how the emission data product was developed within our upgraded emission modeling  
16 framework. Based on CDIAC emission data, ODIAC2016 can be viewed as an extended  
17 version of CDIAC gridded data with improved emission spatial distributions representations.  
18 Utilizing the best available data (emission estimates and proxy), we achieved a  
19 comprehensive, global fossil fuel CO<sub>2</sub> gridded emission field that allows data users to impose  
20 their CO<sub>2</sub> simulations in a consistent way with the global carbon budget analysis. With  
21 updated fuel statistics, we should be able to continue producing updated, future versions of  
22 ODIAC emission data product within the same model framework. The capability we  
23 developed in this study has become more significant now, given CDIAC's shutdown. Despite  
24 of expected difficulties (e.g. discontinued CDIAC estimates), the authors believe that ODIAC  
25 could play an important role in delivering emission data to the carbon cycle science  
26 community. Limitations and caveats discussed in this manuscript mirror and lead ODIAC's  
27 future prospects. The ODIAC emission data product is distributed from  
28 <http://db.cger.nies.go.jp/dataset/ODIAC/> with a DOI. Currently we are working on the 2017  
29 version of ODIAC emission data (ODIAC2017, 2000-2016) and expecting to release by fall  
30 2017.

31

32

## 33 Appendix A

34

35 **Table A1.** A list of components in ODIAC2016 and data used in the development.

36

Component	Data/product name	Description and data source	Reference
Global FFCO <sub>2</sub>	CDIAC global fossil-fuel CO <sub>2</sub> emissions	The year 2016 edition of CDIAC global total estimates were used to constrain the ODIAC2016 totals. Data available at <a href="http://cdiac.ornl.gov/ftp/ndp030/global.1751_2013.ems">http://cdiac.ornl.gov/ftp/ndp030/global.1751_2013.ems</a> .	Boden et al. (2016)
National FFCO <sub>2</sub>	CDIAC fossil-fuel CO <sub>2</sub> emissions by Nation	The year 2016 editions of CDIAC national emission estimates are used as a primary input data. Data available at <a href="http://cdiac.ornl.gov/ftp/ndp030/nation.1751_2013.ems">http://cdiac.ornl.gov/ftp/ndp030/nation.1751_2013.ems</a> .	Boden et al. (2016)
Global fuel	BP	The year 2016 edition of BP statistical data were used to	BP (2017)



statistics	Statistical review of world energy	project CDIAC emissions over the recent years (2014-2015). Data are available at <a href="http://www.bp.com/en/global/corporate/energy-economics/statistical-review-of-world-energy.html">http://www.bp.com/en/global/corporate/energy-economics/statistical-review-of-world-energy.html</a> .	
Monthly temporal variation	CDIAC Gridded Monthly Estimate	The year 2013 version of CDIAC monthly gridded data were used to model seasonality in ODIAC2016. Data are available at <a href="http://cdiac.ornl.gov/ftp/fossil_fuel_CO2_emissions_gridded_monthly_v2013/">http://cdiac.ornl.gov/ftp/fossil_fuel_CO2_emissions_gridded_monthly_v2013/</a>	Andres et al. (2011)
NTL (for non-point emissions)	Global Radiance Calibrated Nighttime Lights	Multiple year NTL data are used to distribute nonpoint emissions. Data are available at <a href="https://ngdc.noaa.gov/eog/dmsp/download_radcal.html">https://ngdc.noaa.gov/eog/dmsp/download_radcal.html</a> .	Ziskin et al. (2010)
NTL (for gas flaring)	Global Gas Flaring	Global gas flaring NTL data are specifically used to distribute gas flaring emissions. Data are available at <a href="http://ngdc.noaa.gov/eog/interest/gas_flares_countries_shapefiles.html">http://ngdc.noaa.gov/eog/interest/gas_flares_countries_shapefiles.html</a>	Elvidge et al. (2009)
Int'l ship tracks	EDGAR v4.1	The international marine bunker emission field in EDGAR v4.1 was used. Data are available at <a href="http://edgar.jrc.ec.europa.eu/archived_datasets.php">http://edgar.jrc.ec.europa.eu/archived_datasets.php</a> .	JRC (2017)
Int'l Aviation flight tracks	AERO2k	Data were used to distributed aviation emissions. More details can be find at <a href="http://www.cate.mmu.ac.uk/projects/aero2k/">http://www.cate.mmu.ac.uk/projects/aero2k/</a> .	Eyers et al. (2005)
Weekly and diurnal cycle	TIMES	This was not a part of ODIAC2016, however it is useful to note that this scaling factors can be used to create weekly and diurnally varying emissions. Data are available at <a href="http://cdiac.ornl.gov/ftp/Nassar_Emissions_Scale_Factors/">http://cdiac.ornl.gov/ftp/Nassar_Emissions_Scale_Factors/</a> .	Nasar et al. (2013)

1

2

3

**Acknowledgments**

4 TO is supported by NASA Carbon Cycle Science program (Grant # NNX14AM76G). RJA is  
 5 now retired but this work was sponsored by U.S. Department of Energy, Office of Science,  
 6 Biological and Environmental Research (BER) programs and performed at Oak Ridge  
 7 National Laboratory (ORNL) under U.S. Department of Energy contract DE-AC05-  
 8 00OR22725. The authors would like to thank Chris Elvidge and Kim Baugh at NOAA/NGDC  
 9 for providing the nightlight data. The authors also thank Yasuhiro Tsukada and Tomoko  
 10 Shirai for hosting the ODIAC emission data on the data server at NIES.

11

12

13

**References**

14

15 Andres, R. J., Marland, G., Fung, I., and Matthews, E.: A  $1^\circ \times 1^\circ$  distribution of carbon  
 16 dioxide emissions from fossil fuel consumption and cement manufacture, 1950–  
 17 1990, *Global Biogeochem. Cycles*, 10(3), 419–429, doi:10.1029/96GB01523, 1996.

18

19 Andres R. J., Gregg J. S., Losey, L., Marland, G., and Boden, T.A.: Monthly, global  
 20 emissions of carbon dioxide from fossil fuel consumption. *Tellus B*, 63:309-327.  
 21 doi:10.1111/j.1600-0889.2011.00530.x, 2011.

22



- 1 Andres, R. J., Boden, T. A., Bréon, F.-M., Ciais, P., Davis, S., Erickson, D., Gregg, J. S.,  
2 Jacobson, A., Marland, G., Miller, J., Oda, T., Olivier, J. G. J., Raupach, M. R.,  
3 Rayner, P., and Treanton, K.: A synthesis of carbon dioxide emissions from fossil-fuel  
4 combustion, *Biogeosciences*, 9, 1845-1871, doi:10.5194/bg-9-1845-2012, 2012.  
5
- 6 Andres, R. J., Boden, T. A., and Higdon, D.: A new evaluation of the uncertainty associated  
7 with CDIAC estimates of fossil fuel carbon dioxide emission. *Tellus B Chem. Phys.*  
8 *Meteorol.* 66, 23616, 2014.  
9
- 10 Andres, R. J., Boden, T. A., and Higdon, D. M.: Gridded uncertainty in fossil fuel carbon  
11 dioxide emission maps, a CDIAC example, *Atmos. Chem. Phys. Discuss.*,  
12 doi:10.5194/acp-2016-258, in review, 2016.  
13
- 14 Asefi-Najafabady, S., Rayner, P. J., Gurney, K. R., McRobert, A., Song, Y., Coltin, K.,  
15 Huang, J., Elvidge, C., and Baugh, K.: A multiyear, global gridded fossil fuel  
16 CO<sub>2</sub> emission data product: Evaluation and analysis of results, *J. Geophys. Res.*  
17 *Atmos.*, 119, 10,213–10,231, doi:[10.1002/2013JD021296](https://doi.org/10.1002/2013JD021296), 2014.  
18
- 19 Ballantyne, A. P., Alden, C. B., Miller, J. B., Tans, P. P. and White, J. W. C.: Increase in  
20 observed net carbon dioxide uptake by land and oceans during the past 50 years, *Nature*,  
21 488 (7409), 70-72, 2012.  
22
- 23 Baker, D. F., Doney, S. C. and Schimel, D. S.: Variational data assimilation for atmospheric  
24 CO<sub>2</sub>. *Tellus B*, 58: 359–365. doi:10.1111/j.1600-0889.2006.00218.x, 2006.  
25
- 26 Basu, S., Guerlet, S., Butz, A., Houweling, S., Hasekamp, O., Aben, I., Krummel, P., Steele,  
27 P., Langenfelds, R., Torn, M., Biraud, S., Stephens, B., Andrews, A., and Worthy, D.:  
28 Global CO<sub>2</sub> fluxes estimated from GOSAT retrievals of total column CO<sub>2</sub>, *Atmos. Chem.*  
29 *Phys.*, 13, 8695-8717, doi:10.5194/acp-13-8695-2013, 2013.  
30
- 31 Basu, S., Miller, J. B., and Lehman, S.: Separation of biospheric and fossil fuel fluxes of  
32 CO<sub>2</sub> by atmospheric inversion of CO<sub>2</sub> and <sup>14</sup>CO<sub>2</sub> measurements: Observation System  
33 Simulations, *Atmos. Chem. Phys.*, 16, 5665-5683, doi:10.5194/acp-16-5665-2016, 2016.  
34
- 35 Boden, T. A., Marland, G., and Andres, R. J.: Global, Regional, and National Fossil-Fuel  
36 CO<sub>2</sub> Emissions. Carbon Dioxide Information Analysis Center, Oak Ridge National  
37 Laboratory, U.S. Department of Energy, Oak Ridge, Tenn., U.S.A. doi  
38 10.3334/CDIAC/00001\_V2015, 2015.  
39
- 40 Boden, T.A., G. Marland, and R.J. Andres. 2016. Global, Regional, and National Fossil-Fuel  
41 CO<sub>2</sub> Emissions. Carbon Dioxide Information Analysis Center, Oak Ridge National  
42 Laboratory, U.S. Department of Energy, Oak Ridge, Tenn., U.S.A. doi  
43 10.3334/CDIAC/00001\_V2016  
44
- 45 Boden, T.A., G. Marland, and R.J. Andres. 2017. Global, Regional, and National Fossil-Fuel  
46 CO<sub>2</sub> Emissions. Carbon Dioxide Information Analysis Center, Oak Ridge National  
47 Laboratory, U.S. Department of Energy, Oak Ridge, Tenn., U.S.A. doi  
48 10.3334/CDIAC/00001\_V2017



- 1  
2 Bousquet, P., Ciais, P., Peylin, P., Ramonet, M. and Monfray, P.: Inverse modeling of annual  
3 atmospheric CO<sub>2</sub> sources and sinks 1. Method and control inversion, *J. Geophys. Res.*,  
4 104 (D21), 26161-26178, 1999.  
5  
6 Brioude, J., Angevine, W. M., Ahmadov, R., Kim, S.-W., Evan, S., McKeen, S. A., Hsie, E.-  
7 Y., Frost, G. J., Neuman, J. A., Pollack, I. B., Peischl, J., Ryerson, T. B., Holloway, J.,  
8 Brown, S. S., Nowak, J. B., Roberts, J. M., Wofsy, S. C., Santoni, G. W., Oda, T., and  
9 Trainer, M.: Top-down estimate of surface flux in the Los Angeles Basin using a  
10 mesoscale inverse modeling technique: assessing anthropogenic emissions of CO,  
11 NO<sub>x</sub> and CO<sub>2</sub> and their impacts, *Atmos. Chem. Phys.*, 13, 3661-3677, doi:10.5194/acp-13-  
12 3661-2013, 2013.  
13  
14 BP: Statistical Review of World Energy, available at  
15 [http://www.bp.com/en/global/corporate/energy-economics/statistical-review-of-world-](http://www.bp.com/en/global/corporate/energy-economics/statistical-review-of-world-energy.html)  
16 [energy.html](http://www.bp.com/en/global/corporate/energy-economics/statistical-review-of-world-energy.html) (last access: 6 June 2017), 2017.  
17  
18 Chevallier, F., et al.: CO<sub>2</sub> surface fluxes at grid point scale estimated from a global 21 year  
19 reanalysis of atmospheric measurements, *J. Geophys. Res.*, 115, D21307,  
20 doi:10.1029/2010JD013887, 2010.  
21  
22 Doll, C. N. H., Muller, J.-P., and Elvidge, C. D. Nighttime imagery as a tool for global  
23 mapping of socioeconomic parameters and greenhouse gas emissions, *Ambio*, 29, 157–  
24 162, 2000.  
25  
26 Elvidge, C. D., Baugh, K. E., Dietz, J. B., Bland, T., Sutton, P. C., and Kroehl, H. W.:  
27 Radiance calibration of DMSP-OLS lowLight imaging data of human settlements – a new  
28 device for portraying the Earth’s surface entire, *Remote Sens. Environ.*, 68, 77-88, 1999.  
29  
30 Elvidge, C. D., Imhoff, M. L., Baugh, K. E., Hobson, V. R., Nelson, I., Safran, J., Dietz, J. B.,  
31 and Tuttle, B. T.: Night-time lights of the world: 1994-1995, *J. Photogr. Remote Sens.*, 56,  
32 81–99, 2001.  
33  
34 Elvidge, C. D., Ziskin, D., Baugh, K. E., Tuttle, B. T., Ghosh, T., Pack, D. W., Erwin, E. H.,  
35 Zhizhin, M.: A Fifteen Year Record of Global Natural Gas Flaring Derived from Satellite  
36 Data. *Energies*, 2, 595-622, 2009.  
37  
38 Elvidge, C. D., Zhizhin, M., Hsu, F.-C., and Baugh, K. E.: VIIRS Nightfire: Satellite  
39 pyrometry at night, *Remote Sensing*, 5, 4423-4449, 2013a.  
40  
41 Elvidge, C. D., Baugh, K. E., Zhizhin, M., and Hsu, F.-C.: Why VIIRS data are superior to  
42 DMSP for mapping nighttime lights. *Proceedings of the Asia-Pacific Advanced Network*,  
43 35, 62–69. doi: 10.7125/apan.35.7, 2013b.  
44  
45 EPA: Emissions and Generation Resource Integrated Database (eGRID), available at  
46 <https://www.epa.gov/energy/emissions-generation-resource-integrated-database-egrid>  
47 (last access: 6 June 2017), 2017  
48



- 1 Eyers, C. J., Norman, P., Middel, J., Plohr, M., Michot, S., Atkinson, K., and Christou, R. A.:  
2 AERO2k Global Aviation Emissions Inventories for 2002 and 2025, QinetiQ/04/001113,  
3 2005.  
4
- 5 Feng, L., Palmer, P. I., Bösch, H., and Dance, S.: Estimating surface CO<sub>2</sub> fluxes from space-  
6 borne CO<sub>2</sub> dry air mole fraction observations using an ensemble Kalman Filter, *Atmos.*  
7 *Chem. Phys.*, 9, 2619-2633, <https://doi.org/10.5194/acp-9-2619-2009>, 2009.  
8
- 9 Feng, L., Palmer, P. I., Parker, R. J., Deutscher, N. M., Feist, D. G., Kivi, R., Morino, I., and  
10 Sussmann, R.: Estimates of European uptake of CO<sub>2</sub> inferred from GOSAT  
11 X<sub>CO<sub>2</sub></sub> retrievals: sensitivity to measurement bias inside and outside Europe, *Atmos. Chem.*  
12 *Phys.*, 16, 1289-1302, doi:10.5194/acp-16-1289-2016, 2016.  
13
- 14 Feng, S., Lauvaux, T., Newman, S., Rao, P., Ahmadov, R., Deng, A., Diaz-Isaac, L. I., Duren,  
15 R. M., Fischer, M. L., Gerbig, C., Gurney, K. R., Huang, J., Jeong, S., Li, Z., Miller, C. E.,  
16 O'Keefe, D., Patarasuk, R., Sander, S. P., Song, Y., Wong, K. W., and Yung, Y. L.: Los  
17 Angeles megacity: a high-resolution land-atmosphere modelling system for urban  
18 CO<sub>2</sub> emissions, *Atmos. Chem. Phys.*, 16, 9019-9045, doi:10.5194/acp-16-9019-2016,  
19 2016.  
20
- 21 Feng, L., Palmer, P. I., Bösch, H., Parker, R. J., Webb, A. J., Correia, C. S. C., Deutscher, N.  
22 M., Domingues, L. G., Feist, D. G., Gatti, L. V., Gloor, E., Hase, F., Kivi, R., Liu, Y.,  
23 Miller, J. B., Morino, I., Sussmann, R., Strong, K., Uchino, O., Wang, J., and Zahn, A.:  
24 Consistent regional fluxes of CH<sub>4</sub> and CO<sub>2</sub> inferred from GOSAT proxy  
25 XCH<sub>4</sub>: XCO<sub>2</sub> retrievals, 2010–2014, *Atmos. Chem. Phys.*, 17, 4781-4797,  
26 doi:10.5194/acp-17-4781-2017, 2017.  
27
- 28 Ganshin, A., Oda, T., Saito, M., Maksyutov, S., Valsala, V., Andres, R. J., Fisher, R. E.,  
29 Lowry, D., Lukyanov, A., Matsueda, H., Nisbet, E. G., Rigby, M., Sawa, Y., Toumi, R.,  
30 Tsuboi, K., Varlagin, A., and Zhuravlev, R.: A global coupled Eulerian-Lagrangian  
31 model and 1 × 1 km CO<sub>2</sub> surface flux dataset for high-resolution atmospheric  
32 CO<sub>2</sub> transport simulations, *Geosci. Model Dev.*, 5, 231-243, <https://doi.org/10.5194/gmd-5-231-2012>, 2012.  
33  
34
- 35 Ghosh, T., Elvidge, C. D., Sutton, P.C., Baugh, K. E., Ziskin, D., and Tuttle, B. T.: Creating a  
36 Global Grid of Distributed Fossil Fuel CO<sub>2</sub> Emissions from Nighttime Satellite  
37 Imagery. *Energies*, 3, 1895-1913, 2010.  
38
- 39 Gurney, K. R., Law, R. M., Denning, A. S., Rayner, P. J., Baker, D., Bousquet, P., Bruhwiler,  
40 L., Chen, Y. H., Ciais, P., Fan, S., Fung, I. Y., Gloor, M., Heimann, M., Higuchi, K., John,  
41 J., Maki, T., Maksyutov, S., Masarie, K., Peylin, P., Prather, M., Pak, B. C., Randerson, J.,  
42 Sarmiento, J., Taguchi, S., Takahashi, T., and Yuen, C.W.: Towards robust regional  
43 estimates of CO<sub>2</sub> sources and sinks using atmospheric transport models, *Nature*, 415,  
44 626-630, 2002.  
45
- 46 Gurney, K. R., Chen, Y.-H., Maki, T., Kawa, S. R., Andrews, A., and Zhu, Z.: Sensitivity of  
47 atmospheric CO<sub>2</sub> inversions to seasonal and interannual variations in fossil fuel  
48 emissions, *J. Geophys. Res.*, 110, D10308, doi:10.1029/2004JD005373, 2005.



- 1  
2 Gurney, K. R., Mendoza, D., Zhou, Y., Fischer, M., de la Rue du Can, S., Geethakumar, S.,  
3 Miller, C.: The Vulcan Project: High resolution fossil fuel combustion CO<sub>2</sub> emissions  
4 fluxes for the United States, *Environ. Sci. Technol.*, **43**, doi:10.1021/es900806c, 2009.  
5  
6 Gurney K, Razlivanov I, Song Y, Zhou Y. et al. 2012. Quantification of fossil fuel CO<sub>2</sub>  
7 emission on the building/street scale for a large US city. *Environ. Sci. & Technol.* 46:  
8 12194-12202.  
9  
10 Hakkarainen, J., I. Ialongo, and J. Tamminen (2016), Direct space-based observations of  
11 anthropogenic CO<sub>2</sub> emission areas from OCO-2, *Geophys. Res. Lett.*, 43, 11,400–  
12 11,406, doi:[10.1002/2016GL070885](https://doi.org/10.1002/2016GL070885).  
13  
14 Hogue, S., Marland, E., Andres, R. J., Marland, G., and Woodard, D.: Uncertainty in gridded  
15 CO<sub>2</sub> emissions estimates, *Earth's Future*, 4, 225–239, doi:10.1002/2015EF000343, 2016.  
16  
17 Hutchins, M.G., Colby, J.D., Marland, G. and Marland, E.: A comparison of five high-  
18 resolution spatially-explicit, fossil-fuel, carbon dioxide emission inventories for the  
19 United States, *Mitig Adapt Strateg Glob Change.*, doi:10.1007/s11027-016-9709-9,  
20 2016  
21  
22 Janardanan, R., Maksyutov, S., Oda, T., Saito, M., Kaiser, J. W., Ganshin, A., Stohl, A.,  
23 Matsunaga, T., Yoshida, Y., and Yokota, T.: Comparing GOSAT observations of  
24 localized CO<sub>2</sub> enhancements by large emitters with inventory-based estimates, *Geophys.*  
25 *Res. Lett.*, 43, 3486–3493, doi:[10.1002/2016GL067843](https://doi.org/10.1002/2016GL067843), 2016.  
26  
27 Janssens-Maenhout G, Dentener F, Van Aardenne J, Monni S, Pagliari V, Orlandini L,  
28 Klimont Z, Kurokawa J, Akimoto H, Ohara, T, Wankmueller R, Battye B, Grano D;  
29 Zuber A, Keating T. EDGAR-HTAP: a Harmonized Gridded Air Pollution Emission  
30 Dataset Based on National Inventories. Ispra (Italy): European Commission Publications  
31 Office; 2012. JRC68434, EUR report No EUR 25 299 - 2012, ISBN 978-92-79-23122-0,  
32 ISSN 1831-9424  
33  
34 JRC: EDGAR – Emissions Database for Global Atmospheric Research, available at  
35 <http://edgar.jrc.ec.europa.eu/> (last access: June 2017), 2017.  
36  
37 Kurokawa, J., Ohara, T., Morikawa, T., Hanayama, S., Janssens-Maenhout, G., Fukui, T.,  
38 Kawashima, K., and Akimoto, H.: Emissions of air pollutants and greenhouse gases over  
39 Asian regions during 2000–2008: Regional Emission inventory in ASia (REAS) version 2,  
40 *Atmos. Chem. Phys.*, 13, 11019–11058, doi:10.5194/acp-13-11019-2013, 2013.  
41  
42 Lauvaux, T., et al.: High-resolution atmospheric inversion of urban CO<sub>2</sub> emissions during the  
43 dormant season of the Indianapolis Flux Experiment (INFLUX), *J. Geophys. Res.*  
44 *Atmos.*, 121, doi:[10.1002/2015JD024473](https://doi.org/10.1002/2015JD024473), 2016.  
45  
46 Le Quéré, C., Andrew, R. M., Canadell, J. G., Sitch, S., Korsbakken, J. I., Peters, G. P.,  
47 Manning, A. C., Boden, T. A., Tans, P. P., Houghton, R. A., Keeling, R. F., Alin, S.,  
48 Andrews, O. D., Anthoni, P., Barbero, L., Bopp, L., Chevallier, F., Chini, L. P., Ciais, P.,



- 1 Currie, K., Delire, C., Doney, S. C., Friedlingstein, P., Gkritzalis, T., Harris, I., Hauck, J.,  
2 Haverd, V., Hoppema, M., Klein Goldewijk, K., Jain, A. K., Kato, E., Körtzinger, A.,  
3 Landschützer, P., Lefèvre, N., Lenton, A., Lienert, S., Lombardozi, D., Melton, J. R.,  
4 Metzl, N., Millero, F., Monteiro, P. M. S., Munro, D. R., Nabel, J. E. M. S., Nakaoka, S.-  
5 I., O'Brien, K., Olsen, A., Omar, A. M., Ono, T., Pierrot, D., Poulter, B., Rödenbeck, C.,  
6 Salisbury, J., Schuster, U., Schwinger, J., Séférian, R., Skjelvan, I., Stocker, B. D., Sutton,  
7 A. J., Takahashi, T., Tian, H., Tilbrook, B., van der Laan-Luijkx, I. T., van der Werf, G.  
8 R., Viovy, N., Walker, A. P., Wiltshire, A. J., and Zaehle, S.: Global Carbon Budget 2016,  
9 Earth Syst. Sci. Data, 8, 605-649, doi:10.5194/essd-8-605-2016, 2016.
- 10
- 11 Maksyutov, S., Takagi, H., Valsala, V. K., Saito, M., Oda, T., Saeki, T., Belikov, D. A., Saito,  
12 R., Ito, A., Yoshida, Y., Morino, I., Uchino, O., Andres, R. J., and Yokota, T.: Regional  
13 CO<sub>2</sub> flux estimates for 2009–2010 based on GOSAT and ground-based CO<sub>2</sub> observations,  
14 *Atmos. Chem. Phys.*, 13, 9351-9373, doi:10.5194/acp-13-9351-2013, 2013.
- 15
- 16 Marland, G., and Rotty, R. M.: Carbon dioxide emissions from fossil fuels: a procedure for  
17 estimation and results for 1950–1982. *Tellus B*, 36B: 232–261. doi: 10.1111/j.1600-  
18 0889.1984.tb00245.x, 1984.
- 19
- 20 Myhre, G., Alterskjær, K., and Lowe, D.: A fast method for updating global fossil fuel carbon  
21 dioxide emissions, *Environ. Res. Lett.*, 4, 034012, doi:10.1088/1748-9326/4/3/034012,  
22 2009.
- 23
- 24 Nassar, R., Jones, D. B. A., Suntharalingam, P., Chen, J. M., Andres, R. J., Wecht, K. J.,  
25 Yantosca, R. M., Kulawik, S. S., Bowman, K. W., Worden, J. R., Machida, T., and  
26 Matsueda, H.: Modeling global atmospheric CO<sub>2</sub> with improved emission inventories and  
27 CO<sub>2</sub> production from the oxidation of other carbon species, *Geosci. Model Dev.*, 3, 689-  
28 716, doi:10.5194/gmd-3-689-2010, 2010.
- 29
- 30 Nassar, R., Napier-Linton, L., Gurney, K. R., Andres, R. J., Oda, T., Vogel, F. R., and Deng,  
31 F.: Improving the temporal and spatial distribution of CO<sub>2</sub> emissions from global fossil  
32 fuel emission data sets, *J. Geophys. Res. Atmos.*, 118, 917–933,  
33 doi:10.1029/2012JD018196, 2013.
- 34
- 35 Oda, T., Maksyutov, S., and Elvidge, C. D.: Disaggregation of national fossil  
36 fuel CO<sub>2</sub> emissions using a global power plant database and DMSP nightlight data, *Proc.*  
37 *of the Asia Pacific Advanced Network*, 30, 220-229, 2010.
- 38
- 39 Oda, T. and Maksyutov, S.: A very high-resolution (1 km×1 km) global fossil fuel  
40 CO<sub>2</sub> emission inventory derived using a point source database and satellite observations  
41 of nighttime lights, *Atmos. Chem. Phys.*, 11, 543-556, doi:10.5194/acp-11-543-2011,  
42 2011.
- 43
- 44 Oda, T., Ganshin, A., Saito, M., Andres, R. J., Zhuravlev, R., Sawa, Y., Fisher, R. E.,  
45 Rigby, M., Lowry, D., Tsuboi, K., Matsueda, H., Nisbet, E. G., Toumi, R.,  
46 Lukyanov, A., and Maksyutov, S.: The use of a high-resolution emission dataset in a  
47 Global Eulerian-Lagrangian coupled model, "*Lagrangian Modeling of the Atmosphere*",  
48 AGU Geophysical monograph series, 2012.





- 1  
2 Oda, T. and Maksyutov, S.: Open-source Data Inventory for Anthropogenic CO<sub>2</sub> (ODIAC)  
3 emission dataset, National Institute for Environmental Studies, Tsukuba, Japan.  
4 doi:10.17595/20170411.001, URL: <http://db.cger.nies.go.jp/dataset/ODIAC/>  
5  
6 Oda, T., Ott, L., Topylko, P., Halushchak, M., Bun, R., Lesiv, M., Danylo, O. and Horabik-  
7 Pyzel, J.: Uncertainty associated with fossil fuel carbon dioxide (CO<sub>2</sub>) gridded emission  
8 datasets. In: *Proceedings, 4th International Workshop on Uncertainty in Atmospheric*  
9 *Emissions, 7-9 October 2015, Krakow, Poland*. Systems Research Institute, Polish  
10 Academy of Sciences, Warsaw, Poland, pp. 124-129. ISBN 83-894-7557-X  
11  
12 Oda, T, et al: On the impact of granularity of space-based urban CO<sub>2</sub> emissions in urban  
13 atmospheric inversions: A case study for Indianapolis, IN. *Elem Sci Anth*, 5: 28, DOI:  
14 <https://doi.org/10.1525/elementa.146>, 2017  
15  
16 Olsen, S. C., Wuebbles, D. J., and Owen, B.: Comparison of global 3-D aviation emissions  
17 datasets, *Atmos. Chem. Phys.*, 13, 429-441, doi:10.5194/acp-13-429-2013, 2013.  
18  
19 Peters, W., Jacobson, A. R., Sweeney, C., Andrews A. E., Conway, T. J., Masrie, K., Miller, J.  
20 B., Bruhwiler, L. M., Petron, G., Hirsch, A. I., Worthy, D. E., van der Werf, G. R.,  
21 Randerson, J. T., Wennberg, P. O., Krol, M. C. and Tans, P. P.: An atmospheric  
22 perspective on North American carbon dioxide exchange: CarbonTracker, *PNAS*,  
23 November 27, 2007, vol. 104, no. 48, 18925-18930, 2007.  
24  
25 Peylin, P., Law, R. M., Gurney, K. R., Chevallier, F., Jacobson, A. R., Maki, T., Niwa, Y.,  
26 Patra, P. K., Peters, W., Rayner, P. J., Rödenbeck, C., van der Laan-Luijkx, I. T., and  
27 Zhang, X.: Global atmospheric carbon budget: results from an ensemble of atmospheric  
28 CO<sub>2</sub> inversions, *Biogeosciences*, 10, 6699-6720, doi:10.5194/bg-10-6699-2013, 2013.  
29  
30 Raupach, M. R., Rayner, P. J., and Paget, M.: Regional variations in spatial structure of  
31 nightlights, population density and fossil-fuel CO<sub>2</sub> emissions, *Energy Policy*, 38, 4756–  
32 4764, doi:10.1016/j.enpol.2009.08.021, 2010.  
33  
34 Rayner, P. J., Raupach, M. R., Paget, M., Peylin, P., and Koffi, E.: A new global gridded  
35 data set of CO<sub>2</sub> emissions from fossil fuel combustion: Methodology and evaluation, *J.*  
36 *Geophys. Res.*, 115, D19306, doi:10.1029/2009JD013439, 2010.  
37  
38 Román M. O., and Stokes, E. C.: Holidays in Lights: Tracking cultural patterns in demand for  
39 energy services, *Earth's Future*, doi:10.1002/2014EF000285, 2015.  
40  
41 Saeki, T., Maksyutov, S., Sasakawa, M., Machida, T., Arshinov, M., Tans, P., Conway, T. J.,  
42 Saito, M., Valsala, V., Oda, T., Andres, R. J., and Belikov, D.: Carbon flux estimation for  
43 Siberia by inverse modeling constrained by aircraft and tower CO<sub>2</sub> measurements, *J.*  
44 *Geophys. Res. Atmos.*, 118, 1100-1122, doi:10.1002/jgrd.50127, 2013.  
45  
46 Schneising, O., Heymann, J., Buchwitz, M., Reuter, M., Bovensmann, H., and Burrows, J. P.:  
47 Anthropogenic carbon dioxide source areas observed from space: assessment of regional



- 1 enhancements and trends, *Atmos. Chem. Phys.*, 13, 2445-2454, doi:10.5194/acp-13-2445-  
2 2013, 2013  
3  
4 Shrai, T., Ishizawa, M., Zhuravlev, R., Ganshin, A., Belikov, D., Saito, M., Oda, T., Valsala,  
5 V., Gomez-Pelaez, A.J., Langenfelds, R. and Maksyutov, S.: A decadal inversion of CO<sub>2</sub>  
6 using the Global Eulerian-Lagrangian Coupled Atmospheric model (GELCA): Sensitivity  
7 to the ground-based observation network, *Tellus B: Chemical and Physical Meteorology*,  
8 69:1, 1291158, DOI: 10.1080/16000889.2017.1291158, 2017  
9  
10 Takagi H., Saeki, T., Oda, T., Saito, M., Valsala, V., Belikov, D., Saito, R., Yoshida, Y.,  
11 Morino, I., Uchino, O., Andres, R. J., Yokota, T., and Maksyutov, S.: On the benefit of  
12 GOSAT observations to the estimation of regional CO<sub>2</sub> fluxes, *SOLA*, 7, 161–164, 2009.  
13  
14 Tans, P.P, Fung, I.Y. and Enting, I.G.: Observational constraints on the global atmospheric  
15 CO<sub>2</sub> budget, *Science*, 247, 1431-1438, 1990.  
16  
17 Thompson, R. L., Patra, P. K., Chevallier, F., Maksyutov, S., Law, R. M., Ziehn, T., Laan-  
18 Luijkx, I. T., Peters, W., Ganshin, A., Zhuravlev, R., Maki, T., Nakamura, T., Shirai, T.,  
19 Ishizawa, M., Saeki, T., Machida, T., Poulter, B., Canadell, J. G., and Ciais, P.: Top-  
20 down assessment of the Asian carbon budget since the mid 1990s, *Nature Comm.*, 7,  
21 2016.  
22  
23 Vogel, F., Tiruchittampalam, B., Theloke, J., Kretschmer, R., Gerbig, C., Hammer, S., and  
24 Levin, I. : Can we evaluate a fine-grained emission model using high-resolution  
25 atmospheric transport modelling and regional fossil fuel CO<sub>2</sub> observations?. *Tellus B*, 65.  
26 doi:<http://dx.doi.org/10.3402/tellusb.v65i0.18681>, 2013.  
27  
28 Woodard, D., Branham, M., Buckingham, G., Hogue, S., Hutchins, M., Gosky, R., Marland,  
29 G., and Marland, E.: A spatial uncertainty metric for anthropogenic  
30 CO<sub>2</sub> emissions, *Greenhouse Gas Meas. Manage.*, doi:10.1080/20430779.2014.1000793,  
31 2015  
32  
33 Yokota, T., Yoshida, Y., Eguchi, N., Ota, Y., Tanaka, T., Watanabe, H., and Maksyutov, S.:  
34 Global concentrations of CO<sub>2</sub> and CH<sub>4</sub> retrieved from GOSAT: First preliminary results,  
35 *SOLA*, 5, 160–163, doi:10.2151/sola.2009-041, 2009.  
36  
37 Zhang, X., Gurney, K. R., Rayner, P., Liu, Y., and Asefi-Najafabady, S.: Sensitivity of  
38 simulated CO<sub>2</sub> concentration to regridding of global fossil fuel CO<sub>2</sub> emissions, *Geosci.*  
39 *Model Dev.*, 7, 2867-2874, doi:10.5194/gmd-7-2867-2014, 2014  
40  
41 Ziskin, D., Baugh, K., Hsu, F.-C., Ghosh, T., Elvidege, C.: Methods Used For the 2006  
42 Radiance Lights, *Proc. of the 30<sup>th</sup> Asia-Pacific Advanced Network Meeting*, 131-14, 2010.  
43